A Low-Cost Electromagnetic Tagging Technology for Wireless Identification, Sensing, and Tracking of Objects

by

Richard Ribon Fletcher

B.S., Physics
B.S. Electrical Engineering
September 1988

Submitted to the Program in Media Arts and Sciences,
School of Architecture and Planning,
in partial fulfillment of the requirements for the degree of

MASTER OF SCIENCE IN MEDIA ARTS AND SCIENCES
at the
Massachusetts Institute of Technology
February 1997

Signature of Author _____
Program in Media Arts and Sciences
February 6, 1997

Certified by _____
Neil Gershenfeld
Associate Professor of Media Arts and Sciences
Program in Media Arts and Sciences
Thesis Supervisor

Accepted by _____
Stephen A. Benton
Chairperson
Department Committee on Graduate Studies
Program in Media Arts and Sciences

A Low-Cost Electromagnetic Tagging Technology for Wireless Identification, Sensing, and Tracking of Objects

by

Richard Ribon Fletcher

Submitted to the Program in Media Arts and Sciences,
School of Architecture and Planning,
on January 14, 1997
in partial fulfillment of the requirements for the degree of

MASTER OF SCIENCE IN MEDIA ARTS AND SCIENCES
at the
Massachusetts Institute of Technology
February 1997

Abstract

A technical overview of near-field electromagnetic tagging is presented and described in the context of adding functionality, efficiency, and convenience to the spaces in which we live and work. A survey of all common forms of electromagnetic tagging is given, including shoplifting tags and RF-ID (Radio-Frequency Identification) tags. Focus is given to low-cost electromagnetic tags based solely on electromagnetic material structures. A unifying description of these materials tags is introduced which defines four main functions: identification, sensing, data read/write, and tracking of position/orientation. Encoding information into the material properties of an object is introduced as a means of making new connections between the digital world of electronic appliances and the physical world. Several commercial applications are given. A general theoretical framework to model near-field electromagnetic tagging systems is outlined, and a few new types of tags are presented along with experimental data.

Thesis Supervisor: Neil Gershenfeld, Associate Professor of Media Arts and Sciences

A Low-Cost Electromagnetic Tagging Technology for Wireless Identification, Sensing, and Tracking of Objects

by

Richard Ribon Fletcher

Thesis Readers

Thesis Reader _____

Robert O'Handley
Department of Material Science and Engineering

Thesis Reader _____

Tomas Arias
Assistant Professor
Department of Physics

Acknowledgments

Many people have contributed to this thesis, in one form or another – often without knowing it – in school and outside. I would like to thank all the folks at the MIT Media Lab who have all been very nice to me, and particularly thank all the talented people in my research group – not only for technical help, but also for supporting my good ideas and telling me when my ideas are crap. Most of all, I'd like to thank my advisor Neil Gershenfeld, without whose optimism, endless enthusiasm and trust, I would not have been able to venture as far as I have.

On the personal side, I am grateful to my parents for inspiration, to my friends for moral support, and to Christy for opening my eyes to many things after coming to MIT. I'm still learning ...

Forward

This document should not be considered as a complete description of my work, but rather as work in progress. This Masters thesis is merely a technical sketch, and many details and references have been left out for that reason. It is my intention to include forthcoming results and more specific information in future papers as well as my doctoral thesis. For future reference, any non-proprietary and non-patentable information can also be found on our group web page: physics.www.media.mit.edu

– RF

TABLE OF CONTENTS

Chapter I.

Introduction

As we enter the 21st century, it is not uncommon to refer to this time in history as the "Computer Age" or "Information Age." Certainly in the past decade, dramatic changes in communication and information technology are clearly evident through such things as widespread use of electronic mail, the Internet, and the World-Wide Web. Not only offices but also homes are now connected electronically, with digital information flowing among them; and to provide electrical connectivity to ambulant humans, a great deal of wireless and mobile electronic appliances have also permeated society.

Nevertheless, our electronic appliances are inadequate and inefficient for dealing with our growing demand for convenient communication and access to information. Most people cannot send or receive digital information (e-mail, FAX, images, sound files, video, etc.) outside of their office environment. And since the cost and complexity of most information devices is high, a relatively small proportion of the population has access to them. Therefore we need cheaper and more natural ways to network objects together and allow them to interact with the environment.

Part of the solution to dealing with the information around us is networking. If networking was sufficiently low-cost, then the common objects around us could have a means of communicating with each other. In addition to electronic devices in the workplace or in a factory, such an innovation could be applied to our home life. For example, I would be able to call up my refrigerator from work and ask it to defrost the chicken, or send an e-mail to my microwave oven with the cooking times from a recipe I just read on the Internet. Unfortunately our computers generally cannot communicate with our watches or portable phones, much less with our washing machines or microwave ovens. In addition, if a manufacturer wishes to add features to an appliance, it must have it's own computer with display and I/O devices, instead of sharing the resources of another appliance. This is inefficient in terms of information and in terms of cost. We are just starting to see new products which address this need, such as an e-mail terminal built into a telephone and a television internet browser, but we need network technology that is low-cost and flexible, so information capabilities can also be extended to other objects in the spaces we inhabit. At the MIT Media Lab, this level of networking is being developed by Professor Mike Hawley and the Personal Information Architecture Group.

However, perhaps even more fundamental than networking is the problem of sensing. Before we can have a network, we must have connectivity – not only with other objects but with people as well. Since our world isn't static or hardwired, connectivity means access; this requires a means of wirelessly sensing and identifying the objects and people that come in and out of our local worlds. Unfortunately, computers are quite blind to the physical world with which they must ultimately interact. Present computers lack the rich sensory interactions and related mental processes of humans. Devoid of all senses, our "high-tech" environments are severely handicapped and consequently lack two fundamental abilities: *awareness* of the world and the ability to *react* to it.

In short, the goals of information technology is to create not just information appliances, but information *environments*. Such environment would allow people to have access to information wherever they are. Such environments allow people the freedom to carry out their daily tasks without losing access to information. In fact, Professor Neil Gershenfeld states his future vision of information spaces in terms of the "Information Bill of Rights." Briefly stated, a person should have the right to send and receive information, whenever and wherever he or she pleases, be it on your sofa or on the beach. But in addition, a person should have access to privacy and anonymity if one so chooses. Like humans, objects should be able to communicate with humans as well as with other objects. But to have this freedom – to have the convenience of automatic door entry, automated package delivery, automated manufacturing, automated financial transactions, and automated retailing – we need better and lower-cost sensing technology.

Much of the work at the MIT Media Lab has been devoted to the goal of making computers more useful in order to improve the environments in which we live, play, work, and learning. Many of the technical solutions addressing the need for sensing have been motivated by a human perspective. Successful research has yielded camera-based systems which allow computers to see, identify, and react to objects around them. Other work, for example, has advanced the ability for computers to hear and understand human speech and environmental sounds; and haptic interfaces for sensing touch is starting to be explored.

Despite this existing research, however, it is prudent to explore other sensing technologies outside the human paradigm. As we have learned from the invention of the airplane, it is not always necessary to imitate Nature. Since computer applications are quite diverse and subject to a wide range of constraints, alternate means of sensing and interacting with the physical world is a worthwhile endeavor. The technology presented in this thesis is an example of such sensing technology.

A. Tags

A "tag" is something which can be attached to a person or object and thereby enables an information environments to remotely identify objects and people, track their position, or sense their state. The approach to wireless sensing presented in this thesis involves the use of electromagnetic fields, as opposed to optical means. In general, the information acquired via the tag is then used by some sort of electronic appliance to perform its function. In fact, a tag is a type of lower-level network which allows transfer of ID or sensor information. Since it is not economically practical to implant computers into

common objects such as suitcases, golf clubs, books, or pens, these devices can communicate their information by proxy to more intelligent devices. As such, tags represent the lowest level on the information "food chain," illustrated in Figure 1. This thesis discusses the technology involved to create this bottom layer.

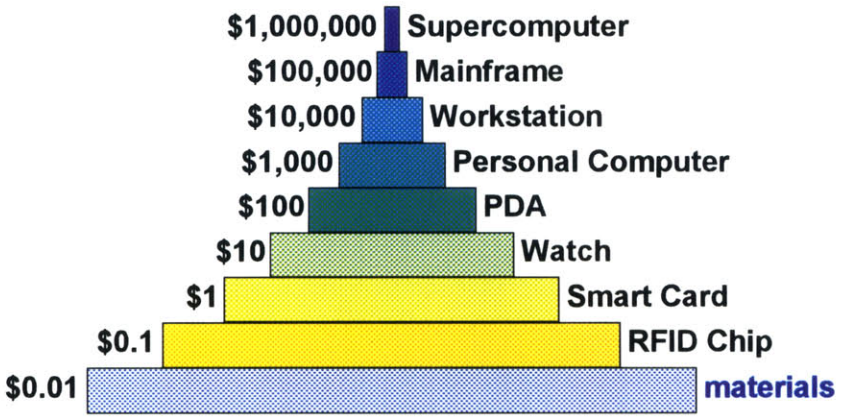

Figure 1. Illustration of "information food chain." As we move down the food chain, the potential number of devices increases dramatically, but lower cost per device is required.

B. Brief Overview of Current Tagging Technology

Tags in the form of radio transponders have existed for at least fifty years. The simplest example is a radio beacon that emits a unique signal which can be detected with a radio receiver at some distance (many meters or more). These are commonly used on all types of aircraft. Other radio tags function as transponders by responding only to a unique signal from a distant transmitter. These tagging systems have been used in a wide variety of applications ranging from wild animal tracking to military surveillance to stolen car retrieval. Such tags are comprised of a radio transmitter powered by some type of battery; naturally, greater battery power is required as the transmitting distance is increased. Other types of tags, such as a diode harmonic tag, simply modulates the transmitted signal which scatters off of it.

Until the 1960's, most of the interest in tagging was in far-field devices, which means that the sensing distance is long compared to the wavelength and to the size of the antennas involved. Although the optical barcode was invented in 1949, it was not until the

mid-1960's that commercial interest began in the field of short-range wireless tagging for shipping, inventory, and retail applications. In 1967, the first commercial barcode scanning systems were installed in supermarkets; and in 1975 the first low-cost electromagnetic tagging systems began appearing in libraries and some retail stores. In the late 1970's a lock company started experimenting with electronic alternatives to the standard key. One group of the company explored a multiple-resonance swept-frequency approach (storing information in the frequency-domain) and the other group explored a chip-modulated fixed frequency approach (encoding information in the time-domain). The swept-frequency approach went on to be developed by Westinghouse for security access applications, and the other idea went on to become what we know today as RF-ID.

The technology known as RF-ID (Radio Frequency Identification) is presently the fastest growing form of near-field electromagnetic tagging. The earliest applications of this technology included tagging cattle and laboratory animals. This type of tag makes use of an electronic chip to communicate with a receiver at some short distance (~ centimeters). In an RF-ID system, the distance between the tag and the base station (known more appropriately as the *tag reader*) is sufficiently small that the signal between them is best characterized by the *coupling* between the tag antenna and the tag reader antenna. In fact, the term *antenna* is somewhat of a misnomer because no far-field transmission is employed as its connotation implies. Parts of the tag and parts of the tag reader are simply coupled together in a manner similar to transformer windings (*inductive coupling*) or as opposing plates in a capacitor (*capacitive coupling*).

The near-field coupling between the RF-ID tag and the reader serves two important functions. First, the coupling is commonly used as a means of supplying power to the tag. If all the necessary electronics inside the tag can be powered remotely from the reader, then the tag requires no local power source. Secondly, since the tag functions as an electrical load on the tag reader, the tag can communicate information to the reader simply by changing the value of its own impedance. The RF-ID tag accomplishes this task through the use of a small electronic chip, which is basically an active switch. As a result, the tag is not required to generate any transmitted signal, and the impedance switching pattern is used to encode the information in the tag. The basic elements of an RF-ID tag is shown schematically in Figure 2. This is not the only way RF-ID tags can function, but it is a common mechanism.

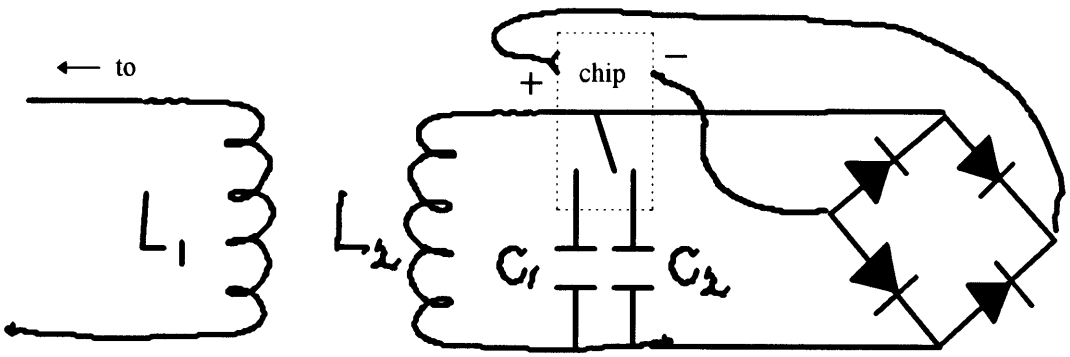

Figure 2. Functional diagram of a tag reader antenna inductively coupled to a battery-less RF-ID tag.

RF-ID tags can be made quite small due to their relative simplicity. For example, RF-ID tags can be embedded inside security badges, which can allow automatic access to secure doors that are equipped with tag readers. RF-ID tags are also embedded into clothing buttons and are used by commercial laundry companies to automatically sort clothing according to each clothing item's ID code.

Although the relative simplicity of the RF-ID circuitry provides a lower-cost alternative to radio tags, any amount of circuitry will always be much more expensive than the most common type of short-distance wireless tagging technology, namely the optical barcode. Since barcodes can be easily printed on a variety of surfaces, barcode tagging technology is extremely cost-effective. However, since reading barcodes requires line-of-sight and some degree of alignment between the barcode and the reader, there exists a certain amount of inefficiency in this approach. As a result, there exists a general desire for the invention of an "electromagnetic barcode" technology which would also be cheap, but would not require line-of-sight. The electromagnetic version of the optical barcode would allow the reader to be hidden behind a wall panel or under a table top. In addition, the electromagnetic transfer of information is generally not affected by operation in dirty environments; and since line-of-sight is not required, tagged objects could be "scanned in" at a faster rate without the need to pause to find the location of the barcode and orient it towards the reader.

C. Low-Cost Alternatives

RF-ID tags can be relatively cheap (~$.90) but optical barcodes are far cheaper (<$.01). Much of the cost of an RF-ID tag is not only due to the electronic chip but – more importantly – to the manufacturing complexity of the entire tag. As a result, the general approach to creating a low-cost electromagnetic tagging technology such as the "electromagnetic barcode" is based on eliminating the electronic chip, and reducing the manufacturing complexity. The challenge, of course, then becomes how best to encode electromagnetic information using materials alone. Since the development of the multiple-resonance frequency tags in the early 1980's, relatively little work has been done outside of RF-ID.

The tagging technology presented in this paper is based on the electromagnetic response of materials. While detecting specific materials electromagnetically is not uncommon – as demonstrated by metal detectors, shoplifting security systems, and medical Magnetic Resonance Imaging systems – it would be useful to create a unified, quantitative and general approach to this topic. By identifying the electromagnetic response of materials, we can view materials as physical representations of information. Furthermore, by knowing how this electromagnetic response depends on the local material environment, materials can also be viewed as remote sensors. The notion that any material structure or object around us can function as a sensor or repository of information can fundamentally change the way we manufacture and package all kinds of products, ranging from military airplanes to pizza boxes to sport shoes.

In terms of cost, material structures thus form a separate class of tagging technology that lies somewhere between RF-ID, magnetic stripe cards, and the optical barcode. Naturally, the cost of a particular tag would depend on the choice of materials and the design of the tag. A description of various materials tag concepts and their corresponding physical description are presented in the following chapters. Some promising potential markets for electromagnetic tagging and practical considerations are discussed in the final chapters, as well as a brief description of ongoing work in our lab.

Chapter II.

The Physics of Tags

A. The Physical Representation of Information

As humans, we experience the world through our senses. As a result, we perceive information as pieces of sound, light, touch, taste, and smell. The ability to stimulate these senses with patterns in frequency, time, and space is what forms our human forms of language. Over the past several decades, however, the increasing "intelligence" of computers and our desire for communication has driven the ability to express information in physical forms which extend beyond our senses. In a simple overseas telephone call, for example, the words "I miss you" may take on a variety of physical forms, in the electronic pulses in the wires and in the microwaves obediently relayed by a communications satellite. Electromagnetic and electro-optic representations of information are now most common, as present-day electronic appliances are increasingly tasked to efficiently communicate with other machines or to sense the physical world around them.

It is most common to conceive of physical matter as the medium through which *dynamic* information is conveyed. The childhood example of communicating across two tin cans attached by a string is now commonly manifested in the form of high-frequency electrical cables or optic fibers. However, information can be *static* as well as dynamic, and the last two decades have produced great advances in information storage media, starting from the simple optical barcode to high-density magnetic and optical media. Although there will always exist material structures optimized for information storage or propagation, it is perhaps more interesting to consider how information may be stored or conveyed in all materials and everyday objects around us.

Most objects around us serve a mechanical purpose – to push, to pull, to cover, to hold. Other objects serve to stimulate our other senses through their appearance – their color, taste, or odor. However, materials possess many other properties which are not always used, namely their electromagnetic properties. By making use of the electromagnetic properties of materials, everyday objects can be empowered to perform the additional functions of storing, conveying, or even generating information. This increased functionality can be achieved through careful design of physical structures within materials; but in the future, perhaps the most elegant approach will be to work directly

with the microscopic properties of the material. In this way, the information function of an object can remain entirely invisible, unless probed by the appropriate electronic instrument. In some ways, the information would be in the eyes of the beholder.

What are the different ways that information can be represented in a material or object? In this document, the answer to this question will be limited to a discussion of wireless electromagnetic mechanisms, which seems to be the most versatile approach, although other approaches are also valid, such as acoustic methods or infrared and millimeter-wave imaging. Just as wireless dynamic information can represented in frequency (e.g. FM radio), time (e.g. TDMA), space (e.g. picocell radio LANs), or a combination thereof (e.g. CDMA), there exist similar analogs for representing information within a material structure. The two basic physical phenomena which are employed, *harmonic generation* and *resonance*, are presented in the sections that follow.

B. Harmonic Generation

Some materials generate harmonics when placed in an electromagnetic field having a particular frequency and amplitude. Harmonic generation is a general term often discussed in a variety of contexts which span the entire electromagnetic spectrum and have a variety of physical origins. For example, materials can exhibit harmonics in their magnetic properties, transport properties, or optical properties. Such materials can be used in applications analogous to those employing non-linear semiconductor electronic devices. Perhaps the most rapidly growing application of such properties can be found in non-linear optical materials which are used to make optical parametric oscillators, phase-conjugate mirrors, and optical computing elements. However, harmonic generation has been perhaps most widely studied in magnetic materials and magnetic devices, such as transformers.

In the electromagnetic tagging of objects, harmonics generated by a soft magnetic material can be used as a means of discriminating the response of the object from the surrounding environment. Some anti-theft tags used for electronic article surveillance have employed this mechanism for at least two decades, and are known as *harmonic tags*. The earliest form of harmonic tag employed a diode as the non-linear element to produce the harmonics. If the tag antenna is tuned to the propagation frequencies, such a tag can be detected at great distances (~ 100 meters). Such tags can be used as a simple way to tag butterflies or people buried in an avalanche.

Most commonly, however, harmonic tags are used in the retail market for ellectronic article surveillance. In its simplest form, a harmonic tag is comprised of a thin strip of magnetic material a few centimeters long. The basic elements of a detection system for such tags is shown in the figure below. The exciter antenna generates magnetic field of a fixed frequency (typically less than 100 Hz) and the receive antenna detects the higher-order harmonics produced by the tag material.

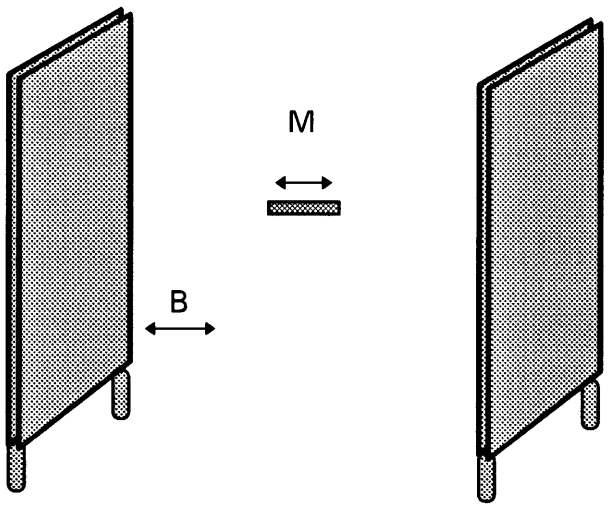

Figure 3. Diagram depicting a harmonic tag between the transmit and receive antennas. Generally, one of the antennas functions as the exciter and the other functions as the pick-up coil.

The harmonics detected by the receive antenna are the result of the magnetic properties of the tag material. More specifically, the induced voltage in the receive coil is due to the changing flux generated by the magnetic field of the transmit coil as well as the magnetization of the tag material. The voltage **V** in the receive coil with N turns and area **A** can be related to the material properties and to the applied field **H** as follows:

$$V = -d\Phi/dt = -Nd/dt\int nB\cdot dA = -d/dt\int(\mu_0 H + M(H))\cdot dA \qquad \text{(Eq. 1)}$$

The amplitude of the detected signal depends on the relative orientations of both antennas as well as the tag. In terms of frequency, it is simple to see that if the magnetization in the material is purely a linear function of the applied magnetic field, then no frequency components would be present other than the frequency of the applied field H. Conversely, if the function M(H) is non-linear over the range of applied field values, then the detected voltage would have harmonic content. For an idealized function M(H) consisting of a step function $\mathbf{u}_{-1}$ of height **m** centered at the origin, then the receive signal would have an infinitely long harmonic spectrum, as can be shown by taking the Fourier transform of the induced voltage:

$$\begin{aligned} F\{V(t)\} &= \int_{-\infty}^{\infty} -\mu_0 N[\int d/dt(H(r,f_0,t)+u_{-1}(H(r,f_0,t))m)\cdot dA]e^{-j2\pi ft}dt \\ &= -\mu_0 N\int_{-\infty}^{\infty}\int d/dt(e^{j2\pi fot}\,H(r)\cdot dA)\,e^{-j2\pi ft}\,dt - NA(m\cdot dA)\int_{-\infty}^{\infty}\delta(t)e^{-j2\pi ft}\,dt \\ &= -\mu_0 N\int_{-\infty}^{\infty}\int 2\pi f_0(e^{j2\pi fot}\,H(r)\cdot dA)\,e^{-j2\pi ft}\,dt - NA(m\cdot dA) \\ &= C_1 f_0\delta(f-f_0) + C_2 \qquad \text{(Eq. 2)} \end{aligned}$$

Here, the time t=0 denotes the time in the M vs H curve at which the applied field H=0. The above result also assumes that the driving field is periodic with single frequency f_0, so that $H(r,\omega_0,t) \propto e^{j2\pi fot}$.

Magnetization curves exhibiting sharp discontinuities can be achieved using magnetically soft alloys. Such curves can resemble step functions but also exhibit hysteresis arising from internal irreversible mechanisms (such as domain wall pinning). In the demagnetized (M=0) state, the magnetic domains will orient themselves along several different energetically favorable directions (usually along a local easy axis). If the material contains local regions with easy axes which are not parallel to the applied field, then the applied field must work harder to align these straggling domains during the magnetization process. This process leads to a rounded magnetization curve. Therefore, crystalline anisotropy is generally not a desired property for achieving a square M vs H loop, except for the special case of a single crystal material with a magnetic field applied along an easy axis.

Applying the excitation field along the easy axis of magnetization can be used to generate a square hysteresis loop similar to the plot shown in Figure 4a. In this configuration, the magnetization process is primarily due to domain wall motion rather than magnetization rotation. For this reason, it is desirable to eliminate all factors which can impede domain wall motion, such as magnetic defects or magnetosctriction, which can produce local strain fields which result in domain wall pinning. Although a small amount of magnetic anisotropy may help to stabilize and maintain the magnetization as the excitation field is reduced from saturation, high anisotropy is generally undesirable since it results in a high domain wall energy density which makes the domain walls more difficult to move.

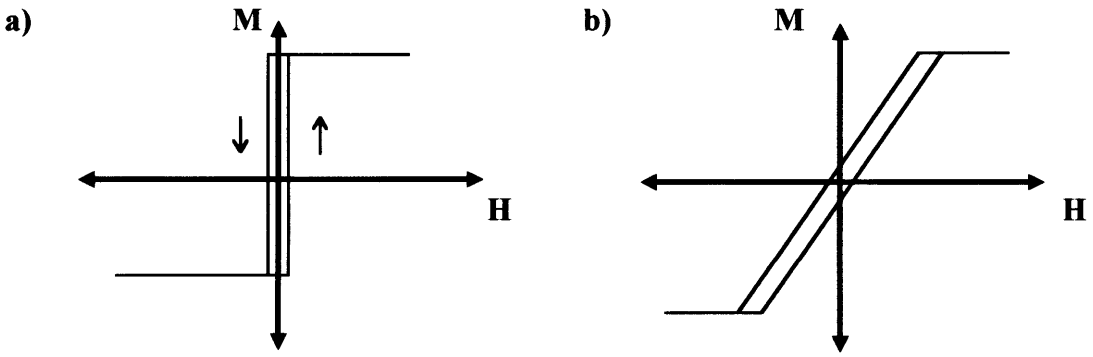

Figure 4. a) M vs H for H applied along the easy magnetic axis
b) M vs H for H appied perpendicular to the magnetic easy axis

Typical soft magnetic materials used for harmonic generation have been Permalloy™, mu-metal, and similar high-permeability materials. For EAS applications, such as for library books or CD's, these materials are generally cut into thin long strips parallel to the easy axis of the material. As expected, the longer the strip, the larger the signal. The long thin geometry is not only convenient for concealment but its thin width and shape anisotropy also help to produce a very square hysteresis loop.

A relatively new class of soft magnetic material are amorphous metal alloys, which were developed in the mid-1970s and are produced by very rapid cooling of the molten alloy. These materials have no crystalline grain structures which can contribute to magnetic anisotropy and domain wall pinning. Perhaps most importantly, these materials exhibit a relatively high electrical resistivity, thus diminishing eddy currents which can impede domain wall motion associated with energy loss in dynamic applications. Now that it is possible to fabricate amorphous metal alloys in thin wire form, amorphous wire has become the material of choice for harmonic tags.

Another method of producing discontinuities in the M vs H curves is to induce a sudden flux jump during the magnetization process by momentarily pinning the movement of one or more domain walls. The pinning regions are created by annealing the material in order to induce local anisotropies at the location of the domain walls present during the annealing process. These pinning regions are in the form of line defects which act as 2D potential wells. The pinning energy of these regions depends on the annealing kinetics (temperature, mobility of the species). The local anisotropies formed during the annealing process are also a function of the chirality of the domain wall, so the pinning energies of these line regions are also chirality-dependent.

The hysteresis loop of a pinned-wall type material and an illustration of its internal domain structure is shown in Figure 5. In its demagnetized state, a narrow strip of this material may have one or more domain walls. As the applied field is increased, the unusual flat sections of the hysteresis loop are the result of domain wall pinning. As the applied field is increased further, eventually enough energy is available to overcome the pinning energy of an existing domain wall or to fully nucleate one of the budding domain walls present at the edge of the material. Once this occurs, the freed domain wall quickly moves to its equilibrium position, thus generating a burst of flux and a step in the M vs H loop.

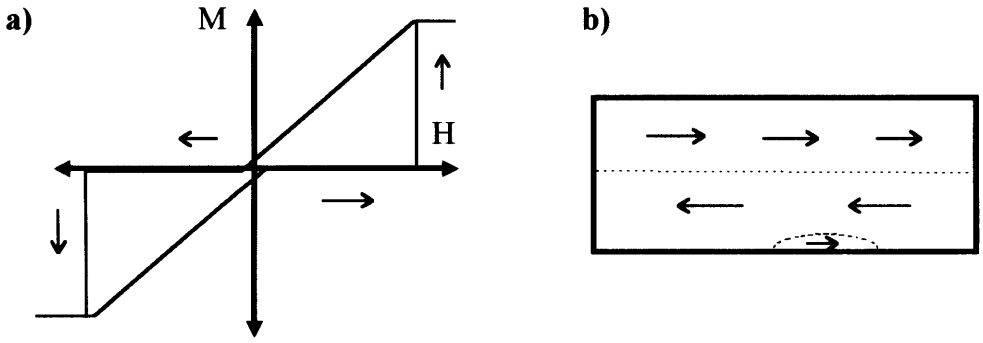

Figure 5. a) Magnetization curve for a pinned-wall material annealed in zero field. b) Diagram of a possible internal domain structure for zero applied field. Domain walls are represented by dotted lines.

If the material is annealed in the presence of a magnetic field, very asymmetric hysteresis loops can be created (Fig 6). Since the potential well regions are formed at the location of the domain walls during the annealing process, the flat sections of the resulting hysteresis loop correspond to the applied field values which reproduce the domain wall configuration during the annealing. It also follows that the value of the magnetization

during pinning (the flat sections of the curve) corresponds to the magnetization value during annealing. As shown in Figure 6, this process can produce large steps in the M vs H loop which have high harmonic content. It should also be noted that this process also provides a way to create an asymmetric step in the M vs H loop located away from the origin (analogous to coercivity) in order to safeguard against accidental activation by small environmental excitation fields.

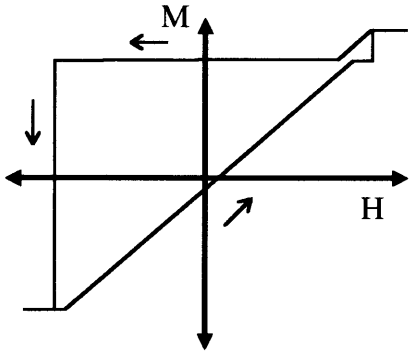

Figure 6. Example of a magnetization loop for a pinned-wall material annealed in a field. Of particular interest is the resulting large step in magnetization.

C. Electromagnetic Resonance

Resonance is a fundamental phenomenon used in electromagnetic tagging. In the following sections, several simple common unifying themes are presented which enable a general approach for measuring and modeling tags containing electromagnetic resonators.

1. What is Resonance?

Resonance is a frequency-dependent stimulated response characterized by a large amplitude response at a specific frequency (or very narrow frequency band). This amplitude response is an indication that a resonant system has the ability to store energy at the resonant frequency. Energy storage in a passive material structure is sustained by a continuous exchange between one form of energy and another. This transfer of energy is sometimes called the circulating power. Energies can be in the form of kinetic energy and potential energy, or expressed in terms of electric fields and magnetic fields, currents and voltages, mechanical stresses and strains, pressure and displacement, or a mixture of these. In order to exhibit a large amplitude response, low internal losses and weak coupling to the external environment are also required. The ratio of stored energy to energy loss per unit cycle defines the quality factor, Q, of the resonator:

$$Q = \frac{W_{TOTAL}}{P/\omega} = \frac{\omega W_{TOTAL}}{P} \qquad \text{(Eq. 3)}$$

where W = total stored energy, P = the average dissipated power, and ω_0 is the resonant frequency.

Resonances are commonly created by constraining the flow of energy out of a physical system as defined by the physical boundary conditions. For example, constraining the ends of a taut violin string gives rise to a discrete set of frequencies that can exist. In an electromagnetic system, the boundary conditions are determined by the spatial dependence of the electromagnetic material properties. In structures having physical dimensions that are on the scale of the electromagnetic wavelength or larger, it is customary to describe resonators as transmission lines with additional boundary conditions added along the direction of propagation. For example, the transverse 2D boundary conditions of a transmission line define a band of frequencies which can propagate, and adding a third boundary condition in the direction of propagation (e.g. by adding metal plates to either end of a metal waveguide segment) will give rise to a discrete set of resonant frequencies.

2. Examples of Resonance

Resonators can be found in many electronic and electromagnetic devices, such as tuning circuits, signal filters, and impedance matching networks. The following is a description of several common types of resonators which are useful in electromagnetic tagging.

a) The LC Resonator

The classic example of a resonant circuit is a series RLC (resistor-inductor-capacitor) configuration (Figure 7a), also known as a tank circuit. The inductor is the magnetic energy storage element, and the capacitor is the electric energy storage element. By considering the flow of current as a function of time, it is easy to see that the magnetic energy is maximum when the electric energy is minimum, and vice versa. Assuming that the resistance in negligible, the current flowing in the resonator (I=V/Z) is maximum when the total impedance, $Z=R+jX \approx jX$, around the circuit is minimum. This occurs when the total reactance $X=X_m+X_e$ is zero, where $X_m = L\omega$ and $X_e = -1/C\omega$. This implies that the resonant frequency occurs at $\omega_0 = 1/\sqrt{LC}$. Of course, the resonance frequency can also be found by solving the differential equations for the circuit with R=0.

A more general result for electromagnetic resonators (even microwave cavities) is simply to say that at resonance, the time-averaged electric stored energy and the magnetic stored energy are equal, so we can also find the resonant frequency as follows:

$$W_m = \frac{1}{2}W_{m\max} = \frac{1}{4}LI_{\max}^2$$

$$W_e = \frac{1}{2}W_{e\max} = \frac{1}{4}CV_{\max}^2 = \frac{1}{4}C\left(\frac{I_{\max}}{C\omega} - I_{\max}R\right)^2 \qquad \text{(Eq. 4)}$$

Assuming that the resistive loss is relatively small such that $R << \frac{1}{C\omega}$ and $R << L\omega$, yields the following result

$$W_m = W_e \Rightarrow \omega \approx 1/\sqrt{LC} = \omega_0 \qquad \text{(Eq. 5)}$$

It is also simple to use these energy quantities to solve for the Q-factor, using the definition given in Equation 3.

$$Q = \frac{W_{total}}{P/\omega_0} = \frac{\omega(W_m + W_e)}{\frac{1}{2}I_{\max}^2 R} = \frac{\omega(2W_m)}{\frac{1}{2}I_{\max}^2 R} = \frac{\omega 2\frac{1}{4}LI_{\max}^2}{\frac{1}{2}I_{\max}^2 R} = \frac{\omega L}{R} \qquad \text{(Eq. 6)}$$

As a practical matter when designing LC resonators, one cannot simply pick a value of L or C and solve for the other to give the desired resonant frequency. Since the electric and magnetic energies have to be comparable, $\frac{1}{2}CV_{\max}^2 \approx \frac{1}{2}LI_{\max}^2$, the voltages and currents need to be considered as well. Therefore, one should first consider the approximate magnitude of the voltages and currents a given system can support (say 20V and 250 mA, for example), and then select appropriate values of both L and C to match. This approach also tends to produce resonators with the highest Q-factors.

In order to solve for the resonant frequency with non-vanishing loss, it is necessary to solve the differential equation for the series RLC circuit:

$$i_L = i_C,\ i_C = -C\frac{dV_C}{dt},\ V_C = L\frac{di}{dt} + iR \Rightarrow LC\frac{d^2i}{dt^2} + RC\frac{di}{dt} + i = 0 \qquad \text{(Eq. 7)}$$

We can assume a complex solution of the form $i = Ae^{j\varpi t} = Ae^{j\omega_r - \omega_i t}$, such that the real part of ϖ $(= \omega_r)$ corresponds to the natural resonant frequency of the system, and the imaginary part of ϖ $(= \omega_i)$ corresponds to the decaying amplitude of the undriven system. Solving for ϖ, gives

$$j\varpi = \frac{-RC \pm \sqrt{(RC)^2 - 4LC}}{2LC} \Rightarrow \varpi = \pm\sqrt{\frac{1}{LC} - \left(\frac{R}{2L}\right)^2} + j\frac{R}{2L} \qquad \text{(Eq. 8)}$$

By observation, equations (6) and (8) can then be combined into a single equation for the complex frequency:

$$\varpi = \pm\sqrt{\omega_0^2 - \left(\frac{\omega}{2Q}\right)^2} + j\frac{\omega}{2Q} \equiv \omega_r + j\frac{\omega}{2Q} \qquad \text{(Eq. 9)}$$

The imaginary component of ϖ is a significant result. It shows that the amplitude of the currents and voltages, as well as the amplitude of the fields, decay exponentially with

time constant $\tau = 2Q/\omega$. Since the energy in a resonator is proportional to the square of the fields, this implies that the energy in a resonator decays with time constant $\tau = Q/\omega$ (since $\left(Ae^{jn}\right)^2 = A^2e^{2jn}$). This is completely consistent with Eq. 3, which relates the Q of a resonator to the stored energy and the rate of energy loss. The Q-factor can then be equivalently defined as the rate at which energy decays in an undriven resonator:

$$W_{TOTAL}(t) = W_{TOTAL}(t=0)e^{-j\omega t/Q} \qquad \text{(Eq. 10)}$$

If we assume the losses are small (but not vanishing) so that Q remains large (Q>>1), then the actual resonant frequency, ω_r, given by the real part of Eq. 9, can be approximated by the ideal lossless resonant frequency, ω_0. In this case, the Q factor can be written as

$$Q = \frac{\omega_r L}{R} \approx \frac{\omega_0 L}{R} = \frac{1}{R}\sqrt{\frac{L}{C}}$$

$$Z = R\left[1 + j\frac{\omega_0 L}{R}\left(\frac{\omega}{\omega_0} - \frac{\omega_0}{\omega}\right)\right] \approx R\left[1 + 2jQ\frac{\omega - \omega_0}{\omega_0}\right] \qquad \text{(Eq. 11)}$$

where Z is the impedance across the circuit.

Eq. 9 and the second part of Eq. 10 are general statements valid for all electromagnetic resonators. However, the expression for the frequency shift $\Delta\omega \equiv \omega_0 - \omega_r$ tends to vary slightly depending on the various approximations used.

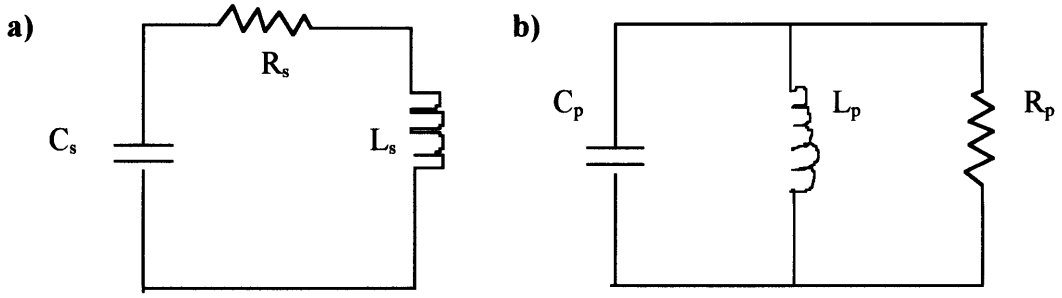

Figure 7. a) series RLC resonant circuit b) parallel RLC resonant circuit

The above derivation can be also applied to a parallel RLC circuit (Figure 7b). In this case the impedance, and hence the voltage, are *maximum* at the resonant frequency, and the current transmitted across the circuit is a *minimum* at the resonant frequency. Working with voltage instead of current as the independent variable, yields the following result:

$$\omega_0 = 1/\sqrt{LC} \text{ and } Q \cong R\sqrt{\frac{C}{L}}$$

$$Y \equiv 1/Z = \frac{1}{R}\left[1 + j\omega_0 CR\left(\frac{\omega}{\omega_0} - \frac{\omega_0}{\omega}\right)\right] \approx \frac{1}{R}\left[1 + 2jQ\frac{\omega - \omega_0}{\omega_0}\right] \qquad \text{(Eq. 12)}$$

where Y is the admittance of across the circuit.

In practice, the dissipated power in a resonator may not be due to a single loss mechanism, such as a single resistor. For example, there may be a dissipative losses associated with the dielectric materials in the capacitor and the magnetic core of the inductor. For the case when there are multiple losses, P_i, it is important to make the following useful observation:

$$Q = \frac{\omega_0 W_{TOTAL}}{\sum P_i} = \left(\frac{\sum P_i}{\omega_0 W_{TOTAL}}\right)^{-1} = \left(\sum Q_i^{-1}\right)^{-1} \qquad \text{(Eq. 13)}$$

This is a very important result which is very useful in modeling all types of resonators. Using this relation, it is possible to start with a simple low-loss model to calculate the Q, and the effect of the other loss mechanisms can be added and compared individually by calculating their corresponding Q values.

b) Metal Cavity Resonators

As the operating frequency of an RLC resonator is increased, the required value of L and C is small, and thus the effect of parasitic inductance and capacitance become increasingly important. As the frequency is increased further, the inductive and capacitive reactances as well as the resistance are distributed (unevenly) throughout the entire structure. As a result, the geometry of the resonator becomes increasingly important, and it becomes necessary to consider the electromagnetic fields of the structure. This evolution is shown in Figure 8.

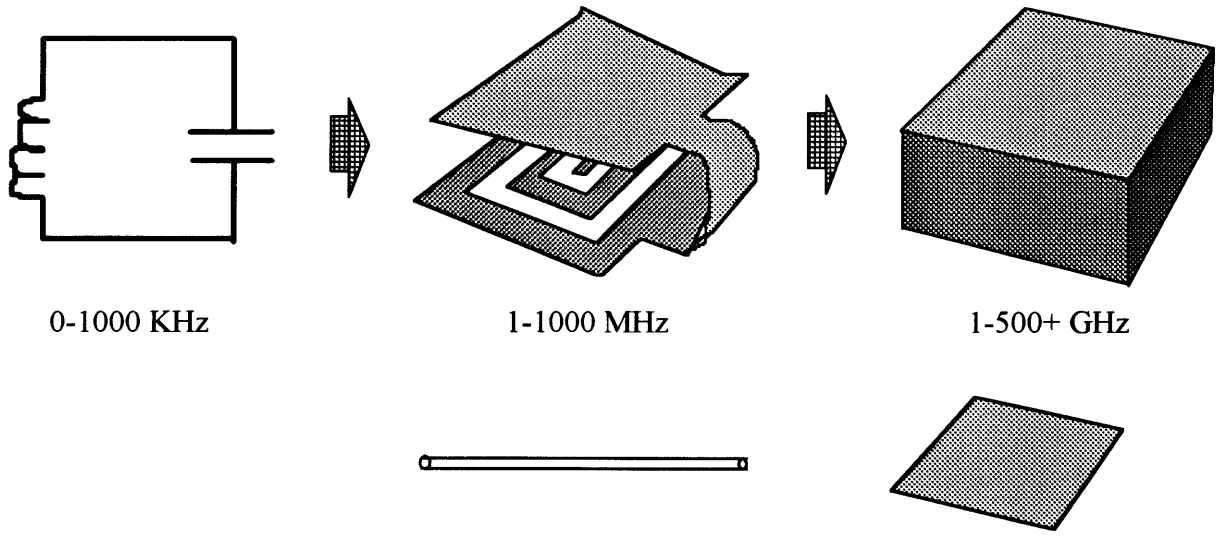

Figure 8. Sketch showing the evolution of an electromagnetic resonator as the operating frequency increases. The bottom row shows 1-D and 2-D variations, a wire resonator and micropatch resonator, respectively.

As the operating frequency is increased still further, 3-dimensional metal and/or dielectric structures are employed to help confine the fields and limit radiation loss. As the wavelength approaches the scale of the resonator dimensions, the resonant frequencies are best found by using the electromagnetic boundary conditions rather than trying to use effective inductance and capacitance values.

The classic example of a high-frequency resonator is a microwave cavity. Other examples would include planar structures such as a patch resonator or a stripline resonator. In a metal cavity, the inductance and magnetic energy arises from the currents flowing on the surface of the metal walls; and the capacitance or electric energy comes from the charge distribution on the walls, which is a maximum when the currents are zero. The dissipative loss in a metal cavity is dominated by the conductive loss in the cavity walls, which is enhanced by the fact that the penetration depth of the currents decrease as the frequency increases.

Because more than one wavelength can fit inside the cavity dimensions and satisfy the boundary conditions, a cavity contains a discrete set of resonant frequencies. These resonances are divided into groups, such as TE (Tranverse-Electric), TM (Transverse Magnetic), or TEM (Transverse Electromagnetic) depending on the respective directions of the electric and magnetic field vectors. Which mode exists in the cavity depends on the operating frequency and depends on the means of excitation. Since it is possible for cavity modes to overlap in frequency (degenerate modes), features are usually added to the cavity walls, either to separate the degenerate modes or to attenuate one mode but not the other. This is part of the art of microwave cavity design.

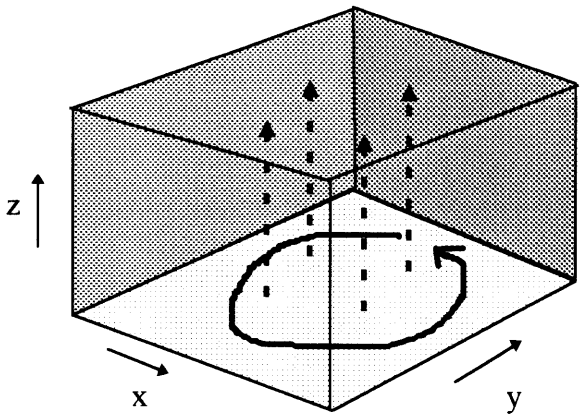

Figure 9. A rectangular metal cavity resonator operating in TE_{101} mode. The magnetic field lines are denoted by a solid arrow line, and the electric field lines are denoted by solid arrow lines.

For a rectangular cavity, shown in Figure 9, it is fairly straightforward to solve for the electromagnetic fields, and will be summarized here for the purpose of illustrating the method to derive the resonant frequency and the Q-factor. Using Maxwell's equations for time-harmonic fields,

$$\begin{aligned} \nabla \times E &= -j\omega\mu H \\ \nabla \times H &= j\omega\varepsilon E + J \\ \nabla \cdot \mu H &= 0 \\ \nabla \cdot \varepsilon E &= \rho \end{aligned} \qquad \text{(Eq. 14)}$$

along with boundary values (e.g. $\sigma=\infty$ on walls), yields the following expressions for the TE_{mnp} modes of a rectangular cavity:

$$E_x = \frac{k_y}{k_0} E_0 \cos k_x x \sin k_y y \sin k_z z \qquad H_x = \frac{j\left(k_x^2 + k_y^2\right)}{\eta k_0^2} E_0 \cos k_x x \cos k_y y \sin k_z z$$

$$E_y = -\frac{k_x}{k_0} E_0 \sin k_x x \cos k_y y \sin k_z z \qquad H_y = \frac{jk_y k_z}{\eta k_0^2} E_0 \cos k_x x \sin k_y y \cos k_z z$$

$$E_z = 0 \qquad H_x = \frac{jk_x k_z}{\eta k_0^2} E_0 \sin k_x x \cos k_y y \cos k_z z \qquad \text{(Eq. 15)}$$

where $\eta = \sqrt{\mu/\varepsilon}$ and $k_0 = \omega\sqrt{\mu\varepsilon}$. The components of the wavenumber vector k must solve the wave equation $\left(\nabla^2 + \omega^2\mu\varepsilon\right)E = 0$ and are constrained by the fact that each of

the cavity dimensions must be an integer multiple of half wavelengths. The result is the following expression for the resonant frequencies:

$$\omega_{mnp} = \frac{1}{\sqrt{\mu\varepsilon}}\sqrt{\left(\frac{m\pi}{a}\right)^2 + \left(\frac{n\pi}{b}\right)^2 + \left(\frac{p\pi}{d}\right)^2} \qquad \text{(Eq. 16)}$$

In order to calculate Q, we make the assumption that the losses in the cavity sufficiently small that the fields in the lossy case do not differ significantly from the fields in the lossless case. Although this criterion seems somewhat arbitrary, the results predicted by this method match observations quite well (within several percent for Q>1000) with errors which decrease as the Q increases. The only quantity which must be calculated is the dissipative loss along the walls of the cavity.

Using the standard definition of Q given earlier, the Q-factor for a given cavity mode is given by the following:

$$Q = \frac{\omega_0 W_{TOTAL}}{P} = \frac{\omega_0\left[\frac{1}{4}\int_V \varepsilon|E|^2 dV + \frac{1}{4}\int_V \mu|H|^2 dV\right]}{\frac{1}{2\sigma\delta}\int_A |n\times H|^2 dA} \qquad \text{(Eq. 17)}$$

where n is the unit surface normal, $\delta = \sqrt{2/\omega\mu\sigma}$ is the skin depth and E and H can be approximated by the expressions for the loss-less fields.

The most general approach to calculating Q and calculating the resonant frequency with losses is to use the notion of the complex frequency mention previously. From Maxwell's equations and Poynting's theorem, the following general expression can be derived for the complex frequency ϖ:

$$\varpi = \frac{j\omega_0\iiint_V\left[\mu_0 H\bullet H_0^* + \varepsilon' E\bullet E_0^*\right]dV - \oiint_S E\bullet K_0^* dS}{j\iiint_V\left[\mu_0 H\bullet H_0^* + \varepsilon' E\bullet E_0^*\right]dV + \iiint_V \varepsilon'' E\bullet E_0^* dV} \qquad \text{(Eq. 18)}$$

where K is the surface current, $\varepsilon = \varepsilon' - j\varepsilon''$ and the subscripts denote the field values with *no loss*. This expression can be rewritten as

$$-j\left(\frac{\varpi-\omega_0}{\omega_0}\right) = \frac{\omega_0\iiint_V\left[\varepsilon'' E\bullet E_0^*\right]dV + \oiint_S E\bullet K_0^* dS}{\omega_0\iiint_V\left[\mu_0 H\bullet H_0^* + \varepsilon' E\bullet E_0^*\right]dV - j\omega_0\iiint_V \varepsilon'' E\bullet E_0^* dV} \qquad \text{(Eq. 19)}$$

If we consider the losses in the cavity to be sufficiently small to that the resulting fields can be approximated by the loss-less fields, then we arrive at the following general result:

$$\frac{1}{Q} = \frac{\frac{1}{2}\mathrm{Re}\left\{\oiint_S E \bullet K^* dS\right\} + \frac{1}{2}\omega_0 \iiint_V \varepsilon'' |E_0|^2 dV}{\frac{\omega_0}{4}\iiint_V \left[\mu_0 |H_0|^2 + \varepsilon' |E_0|^2\right] dV} \qquad \text{(Eq. 20)}$$

$$\frac{\omega_0 - \omega}{\omega_0} = \frac{\frac{1}{2}\mathrm{Im}\left\{\oiint_S E \bullet K^* dS\right\}}{2\frac{\omega_0}{4}\iiint_V \left[\mu_0 |H_0|^2 + \varepsilon' |E_0|^2\right] dV} \qquad \text{(Eq. 21)}$$

where we have made use of the previous relation (Eq. 9), $\varpi = \omega_r + j\frac{\omega_0}{2Q}$. This further shows demonstrates that the complex frequency perturbation approach is a handy way of determining both the unloaded Q and the actual resonant frequency in the presence of losses.

In physical terms, we can consider the small frequency shift $\Delta\omega = \omega - \omega_0$ as due to the fact that electrons have a finite momentum which gives rise to a small phase lag in the field-induced currents. This is expressed as in the surface *reactance* of the walls, in addition to the conducting losses and is also related to the penetration depth. As a result, it is convenient to define a surface impedance for conducting surfaces given by

$$Z_S = \frac{n \times E}{H_{\text{tan}\,gential}} = \frac{n \times E}{n \times J_S} \qquad \text{(Eq. 22)}$$

The surface impedance Z_S is also commonly expressed in terms of the conductivity σ and penetration depth (a.k.a. skin depth) δ as $Z_S = (1+j)/\sigma\delta$.

Since non-ideal walls have a finite penetration depth due to the finite electron momentum, the fields penetrate slightly into the walls, thus resulting in a slightly longer resonant wavelength than in the ideal case. However, in order to calculate the exact reduction in frequency, it is convenient to express the field time-dependence using the complex frequency. Skipping a page of algebra, I will simply state the result:

$$\varpi = \frac{\omega_0}{(1+1/Q - j/Q)^{1/2}} \approx \omega_0\left(1 - \frac{1}{2Q}\right) + j\frac{\omega_0}{2Q} \qquad \text{(Eq. 23)}$$

where ω_0 and Q represent the *particular* lossless resonant frequency and Q factor corresponding to a given mode. This equation can be compared with Eq. 9 of the previous section.

c) Dielectric Resonators

When an electromagnetic wave encounters a boundary between dissimilar media, part of the wave will be transmitted and part will be reflected. The optical propagation properties of a medium are usually characterized by the index of refraction, ***n***, and the relative proportions of the transmitted and reflected waves depend on the degree of dissimilarity between the media as well as the incidence angle of propagation. This phenomena is most familiar to us in optics and can be demonstrated with a simple prism

This phenomenon is actually true for all electromagnetic waves, but it is convenient to express the propagation properties of a material in terms of the permittivity ε and permeability μ rather than the index of refraction. The two representations are related as $n = c\sqrt{\mu'\varepsilon'}$, where c is the speed of light, and where ε' and μ' are the real parts of the complex quantities $\varepsilon = \varepsilon' - j\varepsilon''$ and $\mu = \mu' + j\mu''$. As demonstrated by optic fibers, a material having a value of $\sqrt{\mu'\varepsilon'}$ that is large compared to the surrounding medium can be used to contain or guide a wave. The ability of a material with relatively high ε' or μ' to concentrate the energy of an electromagnetic field can be expressed by the energy expression $E = \frac{1}{8\pi}\int_V \left(\varepsilon' E^2 + \mu' H^2\right) dV$,. In order to function well as a propagation medium, the waveguide material must be insulating and have low dielectric loss (i.e. $\tan\delta \equiv \frac{\varepsilon''}{\varepsilon'} << 1$). As a result, materials with high permittivity are generally used, instead of materials with high permeability.

As in optic fibers, a dielectric waveguide can propagate a band of frequencies which are determined by the geometry and the permittivity of the waveguide. If the ends of the waveguide are cut or terminated in such a way that waves in the dielectric are reflected, then a standing wave condition exists and a resonator is created. In practice, circuits containing dielectric resonators are placed in a metallic enclosure to avoid radiation loss. For cylindrical resonators with dimensions of a few centimeters or less, the resonant frequencies of these structures are in the range of 1 GHz and higher. The miniature size of these structures has been made possible by the ability to manufacture materials with a high dielectric constant (e.g. $\varepsilon \approx 30$) while maintaining a low dielectric loss (e.g. $\tan\delta \approx 10^{-4}$).

As high-frequency resonators, dielectric resonators have several important advantages over metal cavities resonators. Most of the field energy of a dielectric resonator is contained inside the dielectric, so it is not necessary to fabricate a metal enclosure having a low-loss carefully polished surface. For a given resonant frequency, dielectric resonators are smaller and easier to fabricate than an empty or dielectric-filled cavity. Dielectric resonators are much lighter and cheaper ($1 compared to $100) than metal cavities.

Dielectric resonators do have some disadvantages. Their Q-factor ($\leq 10^4$) is smaller than that of the best cavities ($\leq 10^6$ at room temperature), and is limited by $\tan\delta$. Also, the dielectric resonator structures are more complicated to model and design. However, despite these disadvantages, dielectric resonators revolutionized the microwave filter industry in the mid 1970s, particularly in the area of military and commercial communication systems. Each modern communication satellite contains many hundreds of

dielectric resonators. (given that the launch cost alone of a satellite is at least $1000 per pound, can you imagine the size, weight and cost of a satellite containing hundreds of metal cavities?)

The electromagnetic modeling of dielectric resonators is well documented [Kajfez]. Although most resonator configurations require numerical solution, there exist several simple geometries that can be solved in closed form. One such geometry is shown in Figure 10. In order to solve for the resonant frequency and the Q of the resonator, we can use a similar complex power approach used in analyzing the resonators in the previous sections. The following example is taken from a previous paper I co-authored [Fletcher], and the results are summarized here.

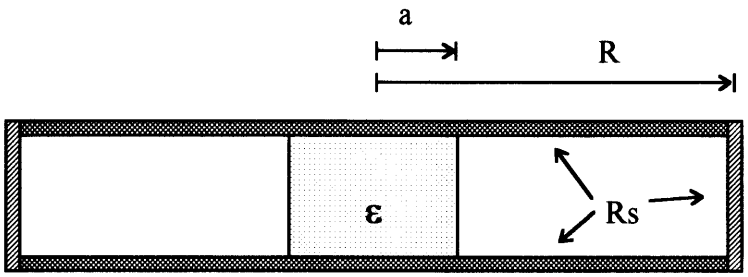

Figure 10. Cross-section view of a cylindrical dielectric resonator and enclosing shield.

If the dielectric loss is relatively small and the surface impedance of the walls is relatively small, then the stored energy of the resonator can be approximated using the electromagnetic fields of the ideal loss-less case. For the TE_{011} mode (which resembles the fields of a magnetic dipole), the non-zero electromagnetic fields can be expressed in cylindrical coordinates by the following:

$$E_\phi(\rho,\phi,z) = jAZ_c M(\rho)\sin\beta_0 z$$
$$H_\rho(\rho,\phi,z) = AM(\rho)\cos\beta_0 z$$
$$H_z(\rho,\phi,z) = AN(\rho)\sin\beta_0 z$$

$$M(\rho) = \begin{cases} J_1(k_u\rho)/J_1(u) & 0 \le \rho \le a \\ \dfrac{K_1(sv)I_1(k_v\rho) - I_1(sv)K_1(k_v\rho)}{K_1(sv)I_1(v) - I_1(sv)K_1(v)} & a \le \rho \le R \end{cases}$$

$$N(\rho) = \begin{cases} -\dfrac{k_u}{\beta_0}\dfrac{J_0(k_u\rho)}{J_1(u)} & 0 \le \rho \le a \\ -\left(\dfrac{k_v}{\beta_0}\right)\dfrac{K_1(sv)I_{01}(k_v\rho) - I_1(sv)K_0(k_v\rho)}{K_1(sv)I_1(v) - I_1(sv)K_1(v)} & a \le \rho \le R \end{cases} \qquad \text{(Eq. 24)}$$

where $k_u = u/a$; $k_v = v/a$; $\beta_0 = \pi/h$; $s = R/a$; $\omega_0 = 2\pi f_0$; $Z_c = \omega_0\mu/\beta_0$; a = radius of dielectric; h = height of dielectric; R = radius of metal cavity enclosure; A = amplitude constant; and the functions J, I, and K are Bessel functions.

For the TE_{011} mode, the parameters u and v are determined by the lowest-order solution to the following simultaneous equations:

$$\frac{J_1(u)}{uJ_0(u)} = \frac{1}{v}\frac{K_1(sv)I_1(v) - I_1(sv)K_1(v)}{K_1(sv)I_0(v) + I_1(sv)K_0(v)}$$

$$u = \sqrt{(\varepsilon_r - 1)\left(\frac{\pi a}{h}\right)^2 - \varepsilon_r v^2} \qquad \text{(Eq. 25)}$$

The resonant frequency for this loss-less case is calculated from the parameter v:

$$\omega_0 = \frac{\pi c}{a}\sqrt{\left(\frac{a}{h}\right)^2 - \left(\frac{v}{\pi}\right)^2} \qquad \text{(Eq.26)}$$

where c is the speed of light in vacuum.

The resonant frequency and the Q-factor for the case with finite loss can then be calculated using a perturbation technique based on the complex frequency. The following equations give the resonant frequency and Q in terms of the fields:

$$\frac{1}{Q} = \frac{(1/2)\oiint_S R_S|K|^2 dS}{2\omega_0 W_E} + \frac{(1/4)\varepsilon_0 \iiint_V \tan\delta\varepsilon_r |E|^2 dV}{W_E}$$

$$\frac{\omega_0 - \omega}{\omega_0} = \frac{(1/4)\oiint_S X_S|K|^2 dS}{2\omega_0 W_E} \qquad \text{(Eq. 27)}$$

where surface current $K = n \times H$ and $W_E = \frac{1}{4}\varepsilon_0 \iiint_V \varepsilon_r |E|^2 dV$ and the fields used are the fields for the lossless case. This result can be compared with Eqs 23 & 24 for the case of a metal cavity.

Finally, evaluating these integrals leads to the following closed-form solution in terms of all the relevant material properties:

$$\frac{1}{Q} = \frac{R_S(2 + C_S)}{G} + \frac{\varepsilon_r \tan\delta}{\varepsilon_r + W}$$

$$\frac{f_0 - f}{f_0} = \frac{X_S(2 + C_S)}{2G} \qquad \text{(Eq. 28)}$$

where

$$G = 480\pi^2\Omega\left(\frac{hf_0}{c}\right)^3\left(\frac{\varepsilon_r + W}{1+W}\right)$$

$$C_S = \frac{1}{\pi^2 s(1+W)}\left(\frac{h}{a}\right)^3\left(\frac{J_1^2(u)}{J_1^2(u) - J_0(u)J_2(u)}\right)\frac{1}{F_1^2(v)}$$

$$W = \left(\frac{J_1^2(u)}{J_1^2(u) - J_0(u)J_2(u)}\right)\frac{F_0^2(v) - F_1^2(v) - (2/v)F_0(v)F_1(v) - (1/v^2)}{F_1^2(v)}$$

and

$$F_0(v) = K_1(sv)I_0(v) + I_1(sv)K_0(v)$$
$$F_1(v) = K_1(sv)I_1(v) + I_1(sv)K_1(v)$$

The case of a non-homogeneous but piece-wise continuous conducting enclosure is also solvable in closed form and is contained in the previously mentioned paper [Fletcher].

d) Magneto-mechanical Resonators

Magneto-mechanical resonators are very different from the resonators mentioned in the previous sections. This type of resonator employs a mechanical resonance that can be excited with a magnetic field and is best described in terms of the basic physics and material science of these resonators. Since the magnetic properties of materials are strongly dependent on their electronic structure, the magnetic and mechanical properties of materials are coupled. In most materials, this coupling is very weak; however, many materials, including iron, exhibit measurable coupled magnetic and mechanical properties. Creating a magnetization in a material can produce an anisotropic strain (magnetostriction) and, conversely, applying a strain on the material can produce a change in its magnetization properties (piezomagnetism). This general class of phenomena are termed *magnetoelastic* effects and coupling between the magnetic and mechanical properties of a material is most commonly characterized by the magnetosctrictivity, d (change in magnetization per unit strain), and the magnetomechanical coupling factor, k (ratio of energy coupling between magnetic modes and elastic modes). The saturation magnetostriction, λ_s, is defined from the measured longitudinal and transverse strains when the material is in the fully magnetized state (see Figure 12b).

The physical origin of magnetoelasticity is a function of a material's macroscopic shape and microscopic electronic structure, which are in turn dependent on the composition and processing of the material. The conditions which cause magnetoelasticity are best described in terms of energy, and a deformation is said to be energetically favorable if it results in a net decrease in the total magnetic and elastic energies. For anisotropic

magnetostriction, it is appropriate to consider the magnetic anisotropy energy which is the change in free energy as a function of the rotation angle of the magnetization about a given axis. The three main contributions to the magnetic anisotropy energy are: magnetostatic energy (due to shape anisotropy), magnetocrystalline anisotropy, and magnetoelastic anisotropy.

Generally, the magnetoelastic contribution to the anisotropy energy is overwhelmed by the other two factors. Some materials may have a large saturation magnetostriction, but are not easy to magnetize due to significant magnetocrystalline anisotropy. For example, relatively large strains ($e \approx 10^{-3}$) can be induced in stressed single crystals of $Tb_{0.35}Dy_{0.65}Fe_2$,(a.k.a. Terfenol-D) through the application of a strong field (~kOe). However, in amorphous metal alloys, such as $Fe_{40}Ni_{38}Mo_4B_{18}$, the low magnetocrystalline anisotropy make these materials easy to magnetize (i.e. high permeability); and although their magnetoelastic anisotropy may not be particularly large, the absence of long-range order and small magnetocrystalline anisotropy, allow the magnetoelastic effects to dominate the response. As a result, these materials can achieve magnetoelastic strains of $e \approx 10^{-5}$ in relatively weak fields (~10 Oe). This is why amorphous metals are good candidates for electromagnetic tags and other devices where the material must respond to a weak magnetic field.

For the purpose of electromagnetic tagging, resonators can be made from magnetoelastic materials by incorporating them into a *mechanically*-resonant structure, which can then be remotely excited and detected *magnetically*. However, unlike a standard LC resonator, the observed amplitude vs frequency of a magnetoelastic resonator is dispersive in nature, while the phase vs frequency signal exhibits a single peak (Figure 11). A lumped-element equivalent circuit model explaining the qualitative behavior of a magnetoelastic resonator can be found in the literature [Butterworth]. Also, the magnetomechanical coupling coefficient depends on the absolute value of the magnetic field and is zero if the applied bias field is zero, so a finite bias field is required for operation.

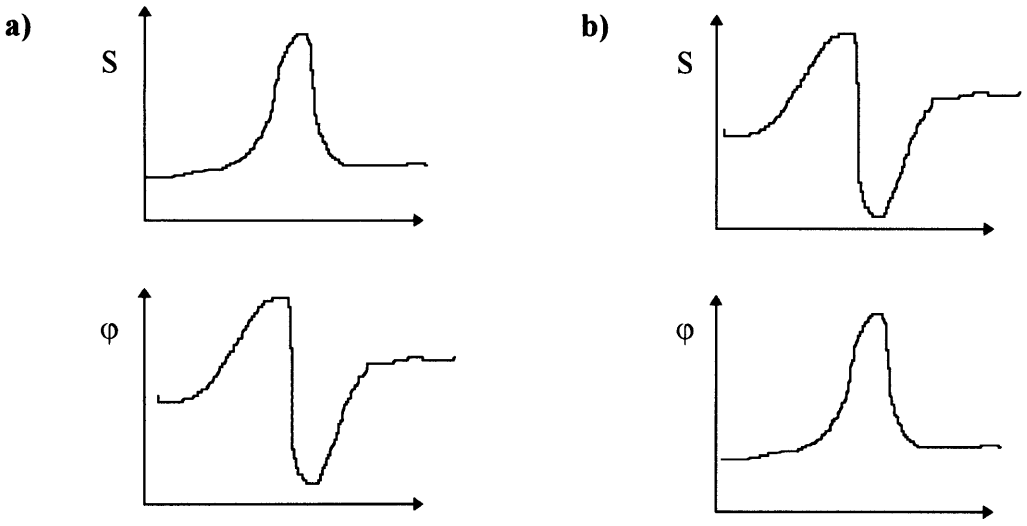

Figure 11. Amplitude S and phase φ as a function of frequency for a) an LC resonator and b) a magnetoelastic resonator.

Amorphous metal ribbons are good candidates for magneto-mechanical resonators for several reasons. Their high yield strength ($>10^8$ N/m^2) makes them resistant to magnetic degradation due to plastic deformation in flexing. In addition, these materials have a relatively high electrical resistivity which limits eddy current losses, and they can be easily tuned to a particular resonant frequency by trimming a strip to the appropriate length given by $f \approx (1/2\pi l)\sqrt{(Y/\rho)}$, where l=length, Y=Young's modulus, and ρ=density. Since the magnetomechanical coupling and the effective modulus of the material can vary with applied magnetic field, the resulting resonant frequency also exhibits some bias-field dependence, with $\Delta f/f \approx 1\%$.

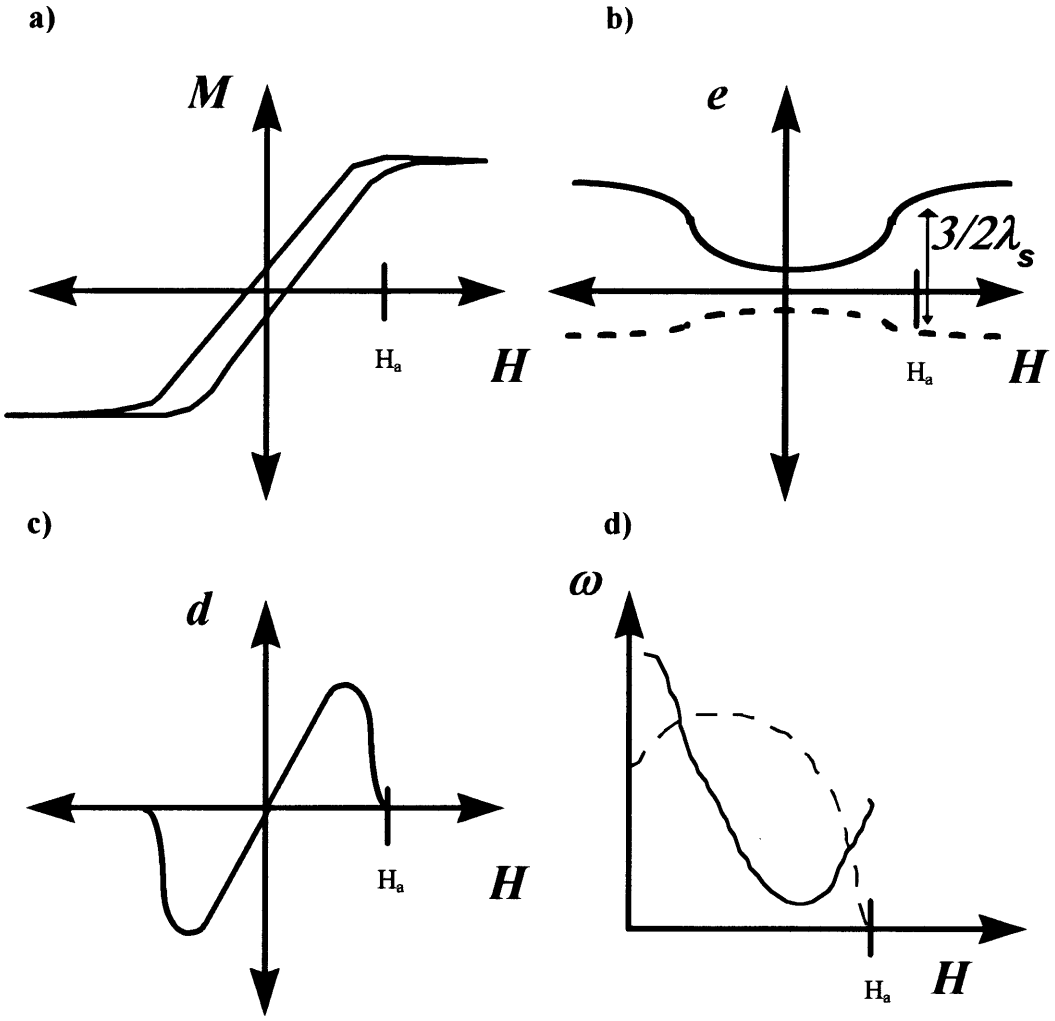

Figure 12. Diagram showing some of the fundamental properties of a strip of magnetoelastic amorphous metal alloy. a) Magnetization curve b) mechanical strain as a function of applied magnetic field; solid line is strain parallel to field, dotted line is strain perpendicular to field. c) magnetostrictivity, $d = \partial e / \partial H$ and d) resonant frequency (solid line) and amplitude (dotted line) as a function of applied magnetic field.

A rather powerful feature of amorphous metal resonators is the ability to control various resonator parameters through annealing of the material. As shown in Figure 12d, the amplitude of the resonance and the bias-field dependence of the resonant frequency can be related to the magnetization curve of the material. As mentioned previously for harmonic tags, the magnetization curve of amorphous materials can be easily modified by annealing in a magnetic field. In a manner similar to other soft magnetic materials, the induced magnetic anisotropy created by annealing produces a sheared M vs H loop after annealing in a transverse field, and produces a squared loop after annealing in a longitudinal field, as shown in Figure 4 for the harmonic materials. However, in this case, we want to avoid inducing an easy axis along the length of the resonant strip, because if

the domains in the M=0 state lie parallel to the applied field, then no domain rotation would take place to produce the desired mechanical strains (180° rotations produce no strain). Similarly, we would expect the greatest mechanical strains from a sample which was annealed in a transverse magnetic field. It should also be noted that the Q of this resonator is limited by the mechanical damping loss of the material (negligible), the eddy current loss, and by the amount and size of the microcrystallites which may form during the post annealing process and produce acoustic losses.

e) Nuclear Magnetic Resonance

Perhaps the most intellectually appealing form of resonance is the type which occurs naturally in the electrons and nuclei of most materials. These phenomena are commonly known as ESR (Electron Spin Resonance) or EPR (Electron Paramagnetic Resonance) and NMR (Nuclear Magnetic Resonance), respectively. Although the frequency of these resonances are a function of the local magnetic field, at a bias field of 1 Tesla, for example, the resonant frequencies occur in the range of several GHz and 50 MHz, respectively. For the purpose or electromagnetic tagging, NMR is more attractive than EPR, because the frequencies below 100 MHz are more easily accessible by consumer electronics, and also because it is already widely used in medical applications to image human tissue.

The physical source of NMR is the magnetic moment arising from the charge, Z, and quantum mechanical spin, I, of nuclei: $\mu=ZeI/2M_nc$, where e is the charge on the electron and c is the speed of light. The application of a static magnetic field, H_0, causes a discrete splitting of the spin energy levels and also defines a direction in space against which projections of the spin angular momentum can be taken. In a macroscopic sample of material, the Boltzmann distribution among these spin energy levels gives rise to a net macroscopic magnetization which can be detected using a coil which applies a sinusoidal magnetic field, H_1, that is transverse to the static field.

If we view the individual spins as magnetic dipoles in an external magnetic field, we see that these spins will precess about the H_0 axis at a rate proportional to the local magnitude of H_0, just as the precession rate of a mechanical toy top is determined by the strength of the local gravitational field. This frequency is given by $\omega= \gamma H$, where γ is defined as the gyromagnetic ratio and depends on the type of nuclei (e.g. $\gamma= 5.586$ for water). When the frequency of the applied transverse field is equal to this precession frequency, the transverse field will apply a net torque on the magnetic dipole which will tip the dipole towards and away from the H_0 axis. Because this signal only appears at a specific frequency, it behaves as a resonance, and it is this time-varying magnetization which is sensed by the magnetic coil as the NMR signal.

It is important to note that the measured resonant frequency is not only dependent on the type of nuclei, but also on the local microscopic magnetic environment. This magnetic environment is dependent on the molecular electronic structure exhibited by the chemical bonding. As a result, materials will generally exhibit a spectrum of resonance peaks indicating not only composition but also bonding geometries. It is this property of NMR which can find potential application in electromagnetic sensing as a means of identifying objects and ascertaining something about its chemical state.

For modeling the signal produced by a coil filled with an NMR material, it is useful to know the complex impedance of the coil, which is given by

$$Z = iL_0\omega(1+4\pi\chi') + L_0\omega 4\pi\chi''+R_0 \qquad \text{(Eq. 29)}$$

where L_0 is the inductance of the empty coil, and the real and imaginary components of the magnetic susceptibility derived from the Bloch equation for magnetization are given by

$$\chi' = -\chi_0'\omega_0 T_2 \frac{(\omega_0-\omega)^2 T_2}{1+(\omega_0-\omega)^2 T_2^{\,2}+\gamma^2 H_1^{\,2} T_1 T_2}$$

$$\chi'' = -\chi_0''\omega_0 T_2 \frac{1}{1+(\omega_0-\omega)^2 T_2^{\,2}+\gamma^2 H_1^{\,2} T_1 T_2} \qquad \text{(Eq. 30)}$$

where χ_0 is the value of the static susceptibility. T_1 is the relaxation time associated with the component of magnetization in the direction of H_0, and T_2 is the relaxation time associated with the transverse component of the magnetization due to the phase coherence of the individual spins.

The complex impedance of the coil allows one to design circuits which contain NMR coils. Some of the basic circuit models which include coupling to an external resonance are described in the following sections.

3. Modeling Resonance

The complex form of Maxwell's Equations for time harmonic waves can be combined with Poynting's Theorem to yield an expression which relates the amount of energy stored in a resonator to the frequency derivatives of the electromagnetic fields (this equation is a variant of the complex frequency equation (Eq. 18) used previously to relate the resonator frequency to the electromagnetic fields):

$$\frac{1}{4}\oint_A\left(\frac{\partial E}{\partial\omega}\times H^* + E^*\times\frac{\partial H}{\partial\omega}\right)\bullet nda = -jw_T - \frac{1}{4}\iiint_V\left(\frac{\partial E}{\partial\omega}\times K^* + E^*\times\frac{\partial K}{\partial\omega}\right)dv$$

(Eq 31)

where $w_T =< w_E > + < w_M >= \frac{\varepsilon'}{4}\int_V E\bullet E^* dv + \frac{\mu'}{4}\int_V H\bullet H^* dv$ is the total electric and magnetic stored energy in the resonator, and K represents the surface current flowing in the resonator, and the power loss in the structure (dissipated+radiated) is defined as

$$P_l = \frac{\sigma}{2}\int_V E\bullet E^* dv + \frac{\omega}{2}\int_V\left(\varepsilon'' E\bullet E^* + \mu'' H\bullet H^*\right)dv + \frac{1}{2}\oint_S \mathrm{Re}\left\{E\times H^*\right\}\bullet dS.$$

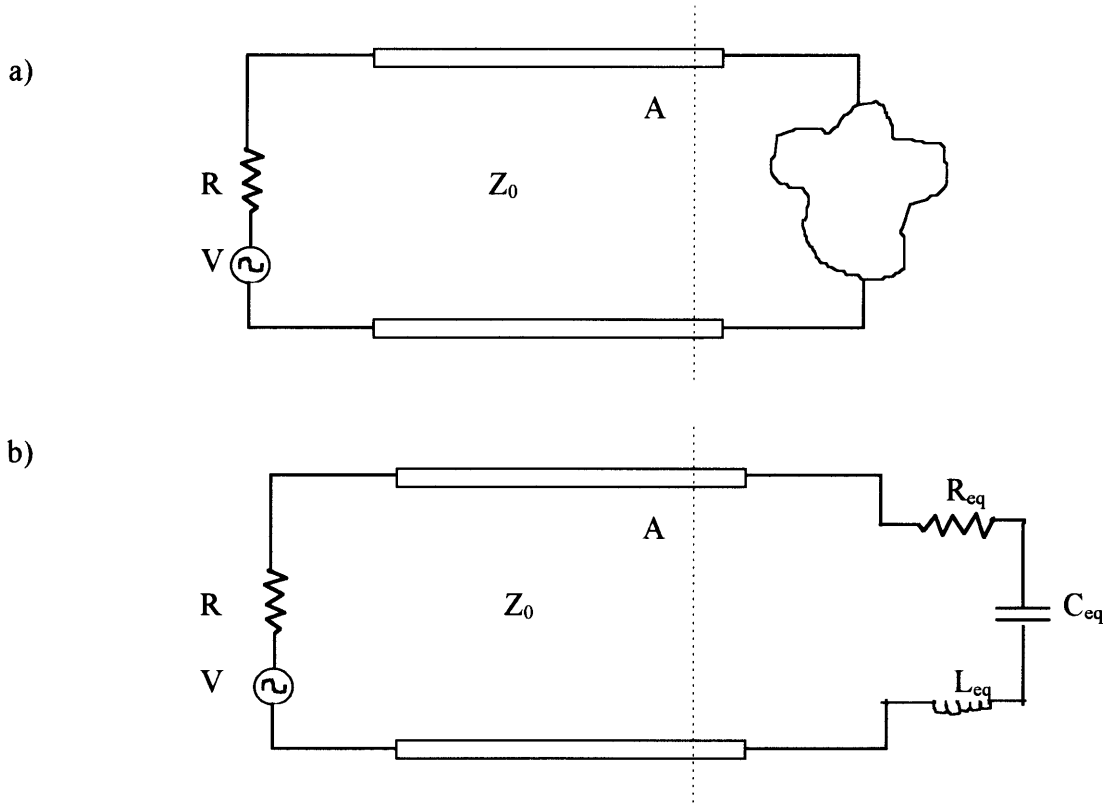

Figure 13. a) An arbitrary resonator connected to the end of a transmission line b) the equivalent circuit model for the resonator at the measurement plane A.

If we consider an arbitrary resonator attached to a transmission line as shown in Figure 13a, we can define the current, I, voltage, V, and impedance $Z=V/I=R+jX$ at a given point A along the transmission line. Since in a lumped element circuit, $< w_E >= \frac{1}{4} CVV^*$, $< w_M >= \frac{1}{4} LII^*$, and $P_l = \frac{1}{2} RII^*$, equivalent L and C could be derived from the stored energies $<w_E>$ and $<w_M>$, and an equivalent R could be derived from the power loss, P_l. By looking at the power flowing in/out or the resonator in terms of the electromagnetic fields and the power in terms of the measured V, I, and Z, it can be shown that the impedance, near the vicinity of the resonance, is given by

$$Z \approx R_{eq} + j \frac{4 < w_T >}{|I|^2} (\omega - \omega_0) \qquad \text{(Eq. 32)}$$

where R_{eq} and I are the resistance and current, respectively, measured at point A along the transmission line.

This result can be compared to the response of a series RLC circuit, presented previously, having impedance Z given by

$$Z = R + j\omega L + \frac{1}{j\omega C} \qquad \text{(Eq. 33)}$$

For frequencies near the resonant frequency, ω_0, this impedance can be expressed as

$$\begin{aligned} Z &= R + j(\omega_0 + \partial\omega)L + \frac{1}{j(\omega_0 + \partial\omega)C} \\ &\approx R + j\omega_0 L - \frac{1}{j\omega_0 C} + j\partial\omega L + \frac{j}{\omega_0^2 C}\partial\omega \\ &= R + 2jL\partial\omega \end{aligned}$$

(Eq. 34)

This result can be compared with Eq. 11 from the previous section. Since for a series LRC resonator, $4w_T / |I|^2 = 2L$, the result for an arbitrary electromagnetic resonator matches that for a series LRC resonator at the point A along the transmission line. Using the relation, $Q = \frac{\omega_0 w_T}{P_d}$, defined previously, it is possible to solve for the equivalent series resistance to L and Q as follows:

$$Q = \frac{\omega_0 < w_T >}{\frac{1}{2} R_{eq} |I|^2} = \frac{\omega_0}{\omega_2 - \omega_1} \equiv \frac{\omega_0}{\Delta\omega} \qquad \text{(Eq. 35)}$$

where ω_2 and ω_1 are the measured frequencies where the power is half of its peak value. For measuring the Q of any system, the equation $Q = \frac{\omega_0}{\Delta\omega}$ is commonly used as a definition of Q.

The equivalent inductance and capacitance can then be derived from the following equations:

$$\begin{aligned} \omega_0 &= \frac{1}{\sqrt{L_{eq} C_{eq}}} \\ L_{eq} &= \frac{2 < w_T >}{|I|^2} = \frac{R_{eq} Q}{\omega_0} \\ C_{eq} &= \frac{1}{\omega_0^2 L_{eq}} = \frac{1}{\omega_0 R_{eq} Q} \end{aligned} \qquad \text{(Eq. 36)}$$

It has been experimentally verified by engineers working with metal cavity resonators, for example, that the power measured at a point very close to the resonator does indeed have the same functional dependence as a series LRC circuit. However, from transmission line theory we know that the measured impedance of a load connected at the end of a transmission line is a function of the position along the line. For example, for a given load Z_L at the end of the transmission line, the impedance measured one quarter wavelength away will be point Z_0^2/Z_L, where Z_0 is the characteristic impedance of the transmission line. As a result, if A is the measurement plane along the transmission line where the resonator impedance resembles a series RLC circuit, then a quarter wavelength away from point A, the circuit will resemble a parallel RLC circuit. As a result, cable length become an important factor at higher operating frequencies.

It will be shown in a later section that an arbitrary resonator which can be modeled as a series RLC circuit will in fact appear as a parallel RLC circuit when inductive or capacitive coupling is used. In practice, when simulating the behaviors of a resonator it is not necessary to find the equivalent series R, L, and C, but rather it is easier to simply work in terms of the measured Q and measured resonant frequency. However, this derivation validates the circuit models which are necessary to relate the unloaded Q and lossless resonant frequency to the measured (loaded) values. For a good easy-to-understand treatment on making a circuit models for general electromagnetic structures, I recommend [Plonsey].

D. Electromagnetically Coupling to a Tag

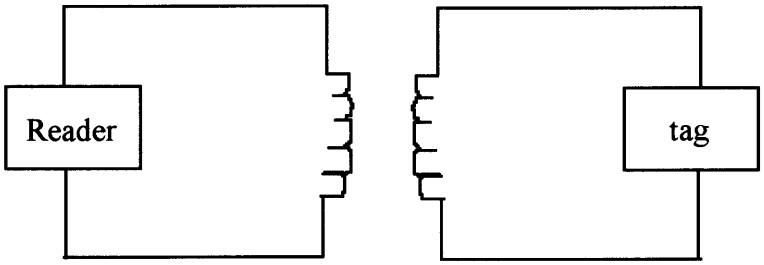

Figure 14. Conventional inductively-coupled tag system.

Conventional materials tag or RF-ID tag systems employ inductive coupling, which is illustrated schematically in Figure 14. In this case, energy is coupled between the reader and the tag via near-field magnetic dipole coupling. In the case of RF-ID, the reader transmits an excitation signal which is used by the electronic chip on the tag as an information signal as well as a source of power. The tag relays its information to the reader simply by changing its input impedance, or in some RF-ID systems by transmitting back a tiny voltage signal. Tag readers can be designed to detect both of these types of signals.

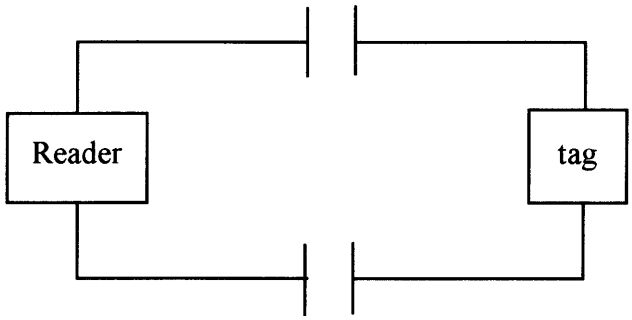

Figure 15. Schematic illustrating a capacitively-coupled tag system.

In the case of the capacitively-coupled tag system, the coupling mechanism is dominated by electric field interactions. The schematic of such a system is shown in Figure 15. The voltage across the reader electrodes induce a voltage across the tag electrodes. Since no large currents are required to generate magnetic fields, such a system is compatible with high-impedance low-power devices. In addition, no coils are needed, and the conductivity of the electrode materials is less critical. The coupling strength is dominated by the amount of charge that can be assembled on the electrodes, rather than the velocity of these charges (i.e. current), so the tag antenna can be comprised of printed conducting patches on paper, for example. As a result, a capacitively-coupled tag system has the potential advantages of having low-power, low manufacturing cost, and low-materials cost. The disadvantages of such a system is environmental interference which is more evident in electric fields than magnetic fields. These issues will be discussed in the following sections.

It should also be pointed out that electrodynamic fields posses both magnetic and electric components, so in any system both types of coupling occur to some extent. For example, in spherical coordinates (with θ defined as the angle from the z-axis), the electric and magnetic fields of a magnetic dipole are given by

$$E(r,\phi,\theta) = -\frac{\mu}{4\pi}\left[\frac{m'(t-r/c)}{r^2} + \frac{m''(t-r/c)}{cr}\right]\sin\theta i_\phi \qquad \text{(Eq. 37)}$$

$$H(r,\phi,\theta) = \frac{1}{4\pi}\left\{2\left[\frac{m(t-r/c)}{r^3} + \frac{m'(t-r/c)}{cr^2}\right]\cos\theta i_r + \left[\frac{m(t-r/c)}{r^3} + \frac{m'(t-r/c)}{cr^2} + \frac{m''(t-r/c)}{c^2 r}\right]\sin\theta i_\theta\right\}$$

(Eq. 38)

where $c = 1/\sqrt{\mu\varepsilon}$, m is the magnetic moment of the small current loop $m = current \cdot area$, and the primes denote time derivatives. The magnetic field has no azimuthal dependence about the dipole axis.

Similarly, the electrodynamic fields of an electric dipole are given by

$$H(r,\phi,\theta) = -\frac{d}{4\pi}\left[\frac{i(t-r/c)}{r^2} + \frac{i'(t-r/c)}{cr}\right]\sin\theta i_\phi \quad \text{(Eq. 39)}$$

$$E(r,\phi,\theta) = \frac{g}{4\pi\varepsilon}\left\{2\left[\frac{q(t-r/c)}{r^3} + \frac{q'(t-r/c)}{cr^2}\right]\cos\theta i_r + \left[\frac{q(t-r/c)}{r^3} + \frac{q'(t-r/c)}{cr^2} + \frac{q''(t-r/c)}{c^2 r}\right]\sin\theta i_\theta\right\}$$

(Eq. 40)

where phase velocity $c = 1/\sqrt{\mu\varepsilon} = \frac{\omega\lambda}{2\pi}$, q is the dipole charge, g is the dipole spacing, and the primes denote time derivatives. The electric field has no azimuthal dependence about the dipole axis.

The dominant form of coupling is determined mainly by the design of the reader and tag antennas. From the expressions for the dipole fields, it is also evident that higher operating frequencies decay more slowly with distance compared to lower frequencies ($\frac{1}{r}$ or $\frac{1}{r^2}$, instead of $\frac{1}{r^3}$). As a result, higher operating frequencies are preferred – but are not sufficient – for applications requiring longer operating distances (read range).

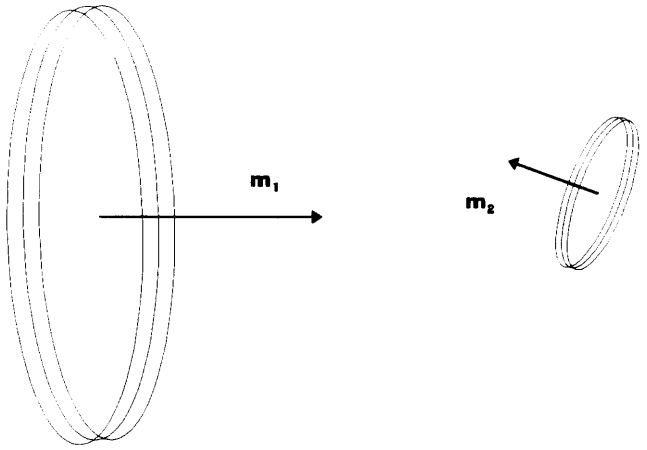

Figure 16. Diagram illustrating the dipole model for a magnetically-coupled tag system. The mutual inductance between two coils, in the far-approximation, is proportional to $\mathbf{m}_1 \bullet \mathbf{m}_2$, where $\mathbf{m}=niA$.

1. Magnetically Coupled Systems

Most of the important performance specifications of a tag system (e.g. read range, orientation dependence, signal to noise ratio, etc.) can be related to the amount of electromagnetic coupling between the tag and reader. For an RF-ID system, if good coupling is present, the other data-related performance factors (e.g. data rate, reading interval, etc.) are then mainly functions of the reader design and the data modulation scheme.

In a conventional inductively-coupled tag systems, the coupling is directly related to the mutual inductance between the reader and tag coils. A circuit model for this system can be made by treating the coupled coils as a transformer inductance with the appropriate turns ratios. If the distance between the reader and tag is relatively short (one the order of the tag diameter), the magnetic coupling between the two coils can be readily calculated from the coil diameters, orientation, and turn ratios. It is also easy to show that the magnitude of the detected signal is proportional to $(\mathbf{d}/\mathbf{D})^3$, where **d** is the diameter of the smaller tag coil and **D** is the diameter of the reader coil.

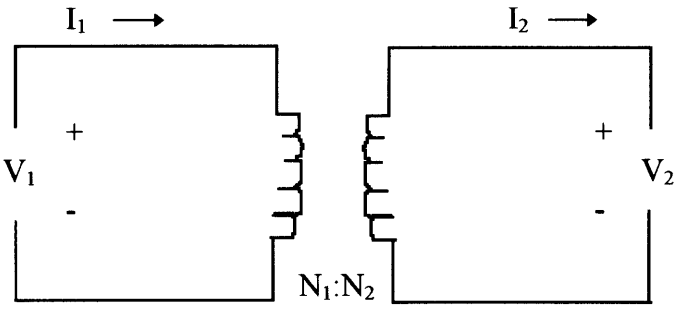

Figure 17. Ideal transformer coupling.

If the tag has a fixed orientation with respect to the reader, we can use the equations for the ideal transformer shown in Figure 17.

$$V_1/ N_1= V_2/ N_2 \text{ and } I_1 N_1= I_2 N_2 \qquad \text{(Eq. 41)}$$

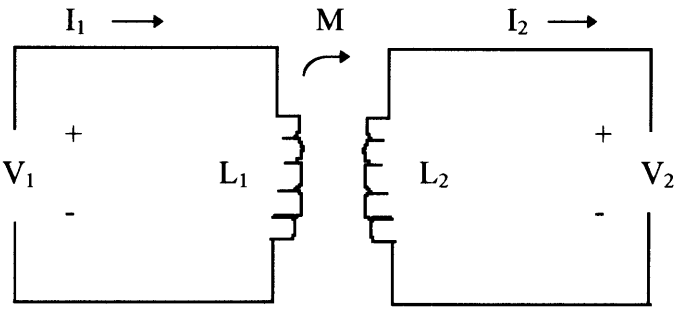

Figure 18. Transformer coupling model using mutual inductance.

If the orientation of the tag is arbitrary but the magnetic fields are known, then it is useful to use the transformer model in terms of the mutual inductance as follows

$$V_1 = j\omega L_1 I_1 + j\omega M I_2$$
$$V_2 = j\omega L_2 I_2 + j\omega M I_1 \qquad \text{(Eq. 42)}$$

where the mutual inductance M between loop 1 and loop 2 is given by

$$M_{21} = \Phi_{21} / I_1 = \frac{1}{I_1} \iint_S B_1 \bullet da_2 \qquad \text{(Eq. 43)}$$

where Φ_{21} is the flux linking coil 1 and coil 2. It should also be noted that in general, $M_{21} = M_{12}$.

If the distance between both coils is much larger than the diameter of the tag coil, it is easier to estimate the mutual inductance by modeling one or both coils as a magnetic dipole **m**, where **m** is the magnetic moment of a given coil and is equal to the total current in the coil multiplied by the area of the coil. The most general approximation is to treat both coils as magnetic dipoles. This is shown in Figure 16. The coupling is then simply proportional to the dot product $\mathbf{m}_1 \bullet \mathbf{m}_2$. This approximation gets poorer as the distance between the coils decreases, particularly if the coils are not coaxial. In these cases, is becomes necessary to actually calculate the magnetic field distribution for at least the reader coil. For example, if the tag coil is much smaller than the reader coil, a useful approximation is to model the tag as a magnetic dipole but to use the full magnetic field distribution of the reader coil.

2. Electrically Coupled Systems

For an electric field coupled system, the coupling mechanism depends on the distribution of charges rather than the distribution of currents. This complicates the task of modeling, since the distribution of free charges in conductors is less well-constrained than currents in loops and generally more difficult to calculate. Assuming the electrodes to be perfect conductors, the primary factors to consider are the sizes and the relative distances between the various electrodes. The circuit model for such a system is shown in Figure 15. As in the previous case of inductive coupling, electromagnetic calculations must be made to solve for the component values used in the circuit model.

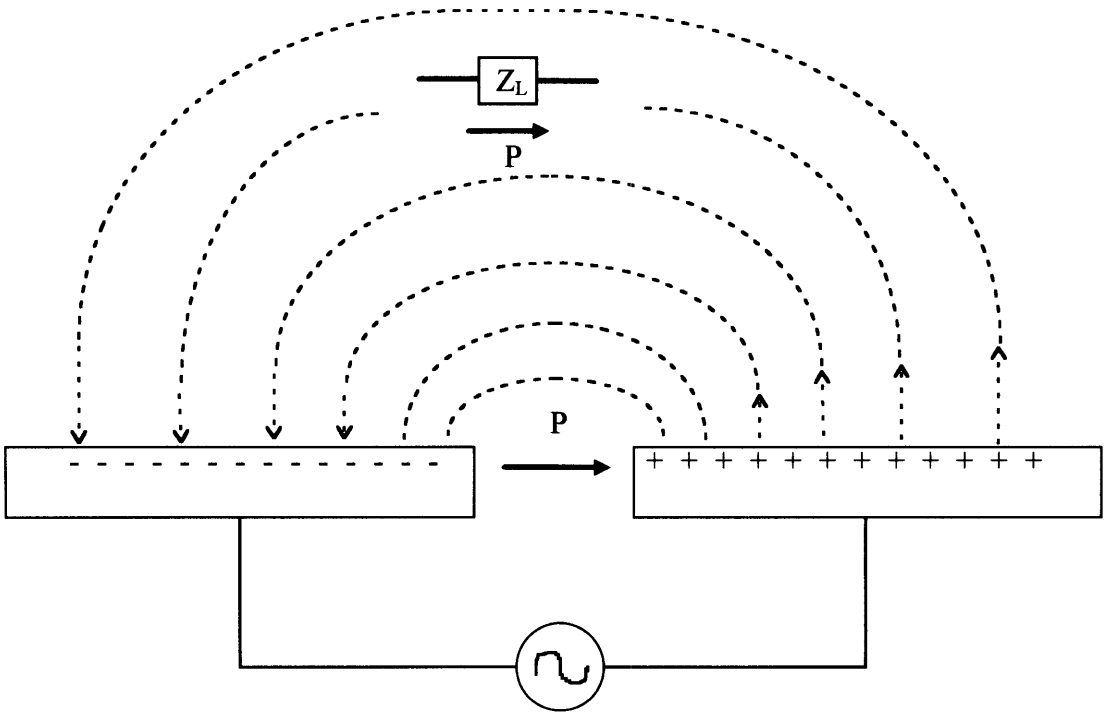

Figure 19. Illustration of the physical geometry of a dipole model for an electrically-coupled tag system.

If the distance between the tag and reader is large compared to the size of the antenna elements on the tag and reader, then it is appropriate to use an electric dipole approximation similar to the magnetic dipole model used for inductive coupling. A dipole field is generated by the reader and coupled to a "dipole" antenna on the tag. As in the magnetic case, the coupling is strongest when the two dipoles are aligned parallel or anti-

parallel. Dipole fields are used since the tag is wireless, has no external source of electrons, and must function without a ground reference. For maximum read range with an RF-ID tag, the chip must redistribute its finite charge in such a way as to create the strongest dipole field with its antenna. The case of electric dipole coupling is shown in Figure 19.

When the tag is in closer proximity to the reader or when the tag electrodes are relatively large, the electric field distribution is dramatically altered and more closely resembles the field of coupled parallel-plate capacitors. Since the tag interacts with a significant portion of the electric field, this mode of coupling is more efficient than dipole coupling and is most appropriate for supplying power to a battery-less RF-ID tag, for example. The case of capacitive coupling is shown in Figure 20. In this case, a coupling model based on a capacitance model is most appropriate. The capacitance between two conducting surfaces in this case is given by

$$C = \frac{Q}{V} = \frac{\iint_S \rho_s dS}{-\int_{r1}^{r2} \vec{E} \bullet d\vec{r}} = \frac{\iint_S \varepsilon(n \bullet E) dS}{-\int_{r1}^{r2} \vec{E} \bullet d\vec{r}} \qquad \text{(Eq. 44)}$$

where Q is the total charge (that is equal and opposite on each plate), ρ_s is the surface charge density, V is the potential difference between the electrodes, E is the electric field distribution between the electrodes and r1, r2 are the positions of the two electrodes.

For the purpose of illustration, Eq. 44 can be applied to the case of two parallel plates having surface area A and small plate spacing d. In this case we can approximate the electric field to be uniform between the plates, the numerator of Eq. 44 is simply εEA, and the denominator is Ed, which leads to the well-known result

$$C = \frac{\varepsilon A}{d} \text{ (Eq. 45)}$$

For other cases where the plates are unequal in size, spaced further apart, or not parallel, various other approximations can be made starting with Eq. 44. A rough approximation is to use a variant of Eq. 45, taking A to be the projected area of the smaller plate on the larger plate.

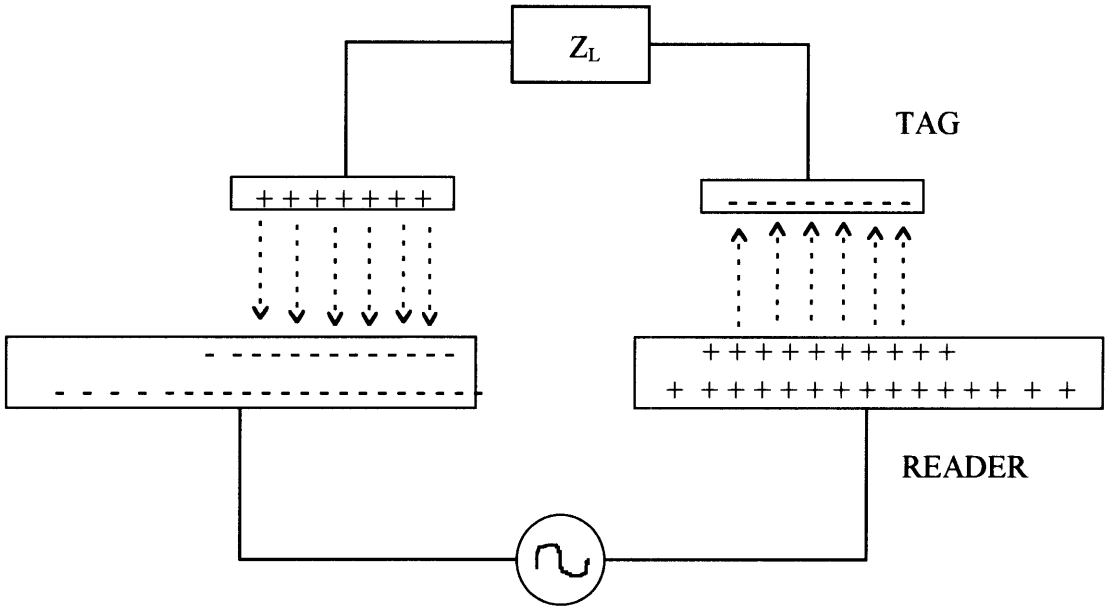

Figure 20. Illustration of the physical geometry of a capacitively-coupled tag system.

E. Tag System Configurations

1. One-port measurement

One method of tag detection is to use a single antenna and measure the amount of power reflected from the tag. This is illustrated in Figure 22. Since both transmission and reception is performed by the same antenna, a directional coupler is typically used in order to isolate the transmitted power from the received signal. If the tag is a resonator with an appreciable Q, then the excitation need not be done continuously, and the pulse-and-ringdown approach mentioned previously could be used.

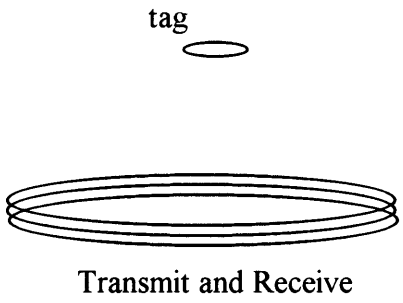

Figure 22. Illustration of 1-port measurement configuration.

The one-port measurement configuration illustrated in Figure 22 can be modeled as follows:

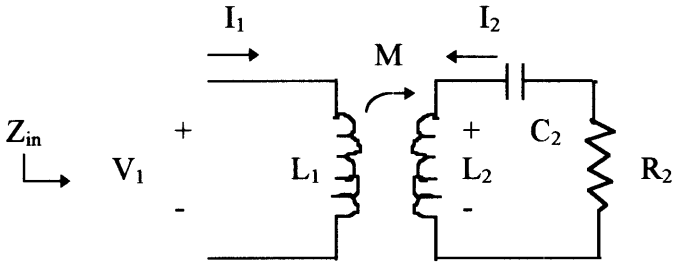

Using the mutual inductance transformer equations given previously (see Eq. 42 and Eq. 43) leads to the following result:

$$V_1 = \left(j\omega L_1 + \frac{\omega^2 M^2}{j\omega L_2 + \frac{1}{j\omega C_2} + R_2} \right) I_1 \qquad \text{(Eq. 46)}$$

$$Z_1 = j\omega L_1 + \frac{\omega^2 M^2}{j\omega L_2 + \frac{1}{j\omega C_2} + R_2} \qquad \text{(Eq. 47)}$$

Making use of the relation $Q = \frac{\omega_0 L_2}{R_2}$, the input impedance can be expressed in terms of the Q-factor:

$$Z_1 = j\omega L_1 + \frac{\omega^2 M^2 / R_2}{1 + jQ\left(\frac{\omega}{\omega_0} - \frac{\omega_0}{\omega}\right)} \qquad \text{(Eq. 48)}$$

If we make the approximation that the losses are small, so that $\frac{\omega_0 - \omega}{\omega_0} << 1$, then we the input impedance Z_1 can be expressed as

$$Z_1 = j\omega L_1 + \frac{R_i}{1 + jQ\frac{2\Delta\omega}{\omega_0}}, \text{ where } R_i \equiv \frac{\omega_0^2}{R_2}. \qquad \text{(Eq. 49)}$$

It should be noted that Eq. 50 could also be written as

$$Z_1 \approx j\omega L_1 + \left(\omega^2 M^2 / R_2\right)\frac{1}{1 + jQ\frac{2\Delta\omega}{\omega_0}} = j\omega L_1 + \frac{1}{j\omega\left(\frac{L_2}{\omega_0^2 M^2}\right) + \frac{1}{j\omega\left(C_2\omega_0^2 M^2\right)} + \frac{R_2}{\omega_0^2 M^2}}$$

(Eq. 50)

This equation is exactly the equation for a parallel LRC circuit in series with an inductor L_1 as shown below:

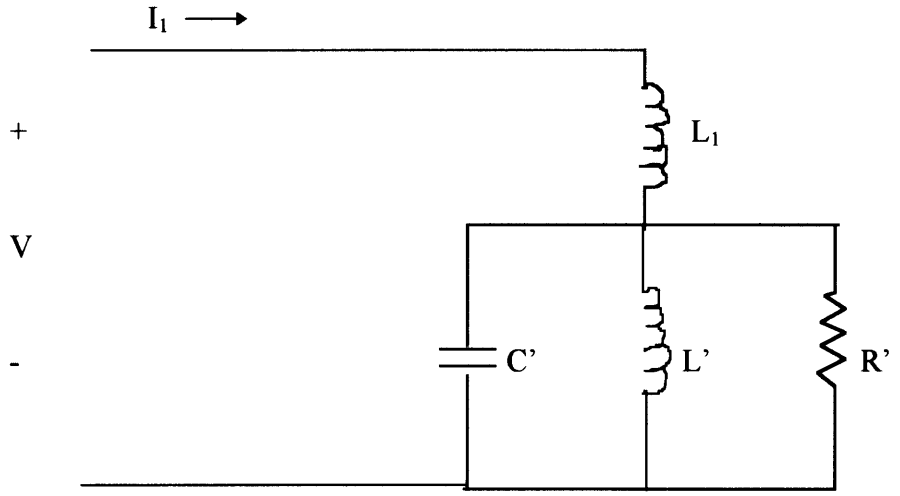

where $C' = \frac{L_2}{\omega_0^2 M^2}$, $L' = C_2 \omega_0^2 M^2$, and $R' = \frac{\omega_0^2 M^2}{R_2}$. This is actually a general result, which shows that all electromagnetic resonators appear as a parallel LRC circuit when inductively coupled to a reader. For greatest measured (loaded) Q, it is generally desirable to keep the series inductance (due to the reader coil) to a minimum. The observed Q can be dramatically lower than the intrinsic (unloaded) resonator Q. The resonator Q and the coupling Q (due to coupling losses) are combined according to Eq. 7 to give the measured Q.

As an aside, it is known that the impedance of a load as measured along a transmission depends on the distance between the measuring point and the load. For a given impedance Z_L atached to the end of a transmission line (see Figure 13), the impedance measured at a distance x away from the load along the line is given by

$$Z_L(x) = Z_0 \frac{(Z_L + Z_0)e^{jkx} + (Z_L - Z_0)e^{-jkx}}{(Z_L + Z_0)e^{jkx} - (Z_L - Z_0)e^{-jkx}} \qquad \text{(Eq. 51)}$$

where Z_0 is the characteristic impedance of the transmission line.

As a brief calculation will show, a quarter wavelength away, a parallel $R_1L_1C_1$ circuit will look like a series circuit with different components $R_2L_2C_2$; and a half wavelength away the circuit will once again look like a parallel $R_1L_1C_1$ circuit; etc. As a result, if the cable length between the reader antenna and the reader is a significant fraction of the wavelength, then the cable length needs to be considered in all the calculations. If the cable length is considerably shorter than one quarter-wavelength, then a one-port inductively-coupled electromagnetic resonator will appear as a parallel resonant circuit.

A one-port tag reader usually works by measuring the reflected power. The reflection coefficient is defined in terms of the input impedance as follows:

$$\Gamma = \frac{Z_{in} - Z_0}{Z_{in} + Z_0} \quad \text{(Eq. 53)}$$

where Z_0 is the characteristic impedance of the reader (typically, Z_0=50 Ohms for lab instruments). Using Eq. 51, the reflection coefficient can then be written as

$$\Gamma = \frac{\left(\frac{R_i}{Z_0} - 1\right) - jQ\frac{2\Delta\omega}{\omega_0}}{\left(\frac{R_i}{Z_0} - 1\right) + jQ\frac{2\Delta\omega}{\omega_0}} \quad \text{(Eq. 53)}$$

For any transmission line having low loss and only inductance per unit length and capacitance per unit length, the characteristic impedance Z_0 will be purely real, so the quantity R_i/Z_0 will be real as well. From this, we can see that the magnitude of the reflection coefficient has a minimum at $\omega=\omega_0$, which matches observation.

On the complex plane, Γ sweeps out a circle as a function of frequency. This circle is centered at $-\frac{Z_0}{R_i + Z_0}$ and with radius $\frac{R_i}{R_i + Z_0}$. In the laboratory, these curves can be conveniently displayed on a normalized complex Γ plane (Smith Chart) using a vector network analyzer. From the Smith chart plot, the resonator parameters as well as the coupling parameters, and type of coupling (overcoupled, undercoupled, critically coupled) can be measured. This is necessary in order to extract the unloaded resonator Q from the measurement of the loaded Q. For the sake of brevity, I will not describe this process, but it can be found in several of the references I have listed. As mentioned previously, it is best to model the impedance of a resonator in terms of ω and Q rather than trying to solve for the equivalent values of R, L, and C.

2. Two-port measurement

Another common detection configuration is the 2-port measurement, illustrated in Figure 22. This is perhaps the easiest configuration to use because a directional coupler is not required and also the transmit and receive antennas can be independently optimized for their respective functions. However, this configuration is more difficult to model than the one-port configuration.

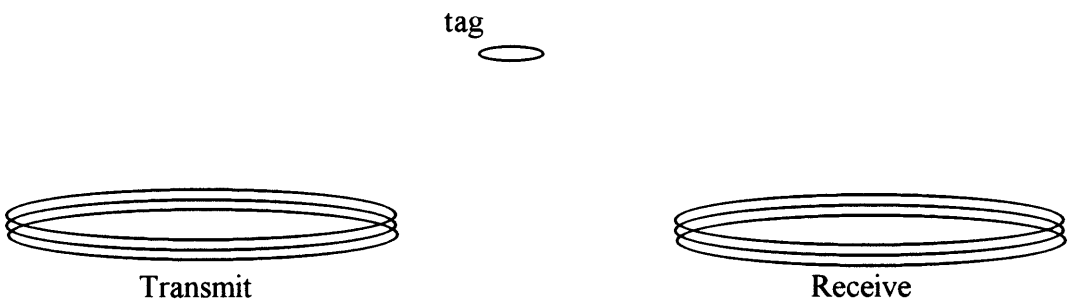

Figure 22. Illustration of 2-port measurement configuration.

Two-port networks can be analyzed in a manner similar to that of one-port networks, but more steps are involved. Instead of measuring the reflection coefficient, Γ, alone and relating it to the Q, in the case of two-port networks, three separate measurements are actually required in order to fully characterize a given network (i.e. the tag, in this case). Instead of Γ, the four S-parameters (S_{11}, S_{22}, S_{21}, S_{12}) are used to characterize the normalized power reflected back or transmitted across the individual measurement ports. (in a reciprocal device, $S_{21}=S_{12}$, so only three measurements are necessary) The measured S-parameters can be used to derive the resonator parameters (unloaded Q and the loss-less resonant frequency, ω_0)as well as the coupling parameters. I will not discuss that here, because there are entire books devoted to subject alone, but I refer the reader to one of my previous papers listed in the references for an example of this process.

Instead of giving a detailed derivation, I will simply provide two examples which illustrate how the transformer equations given previously can be used in transmission lines to model a two-port coupled network. This will provide a general idea of how a two-port measurement can be modeled.

Example 1: Power transferred through resonator tag to receive coil having impedance R_{out}.

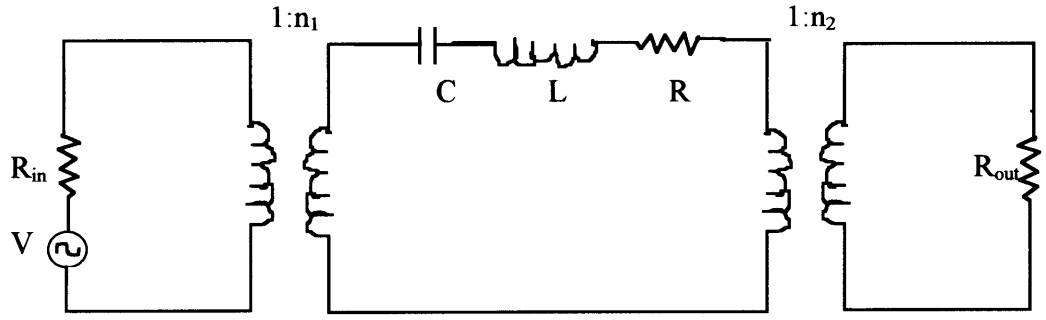

Using the transformer relations, the equivalent circuit becomes

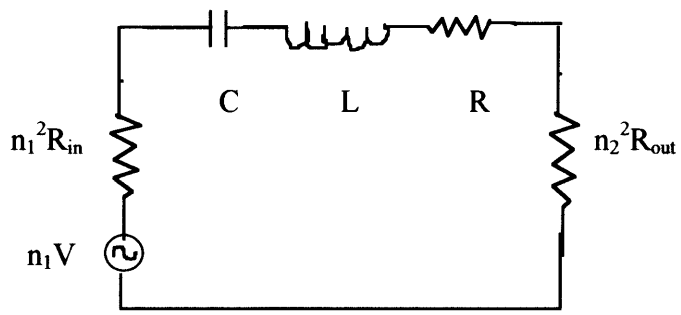

Example 2: the impedance of one port as seen from the other port

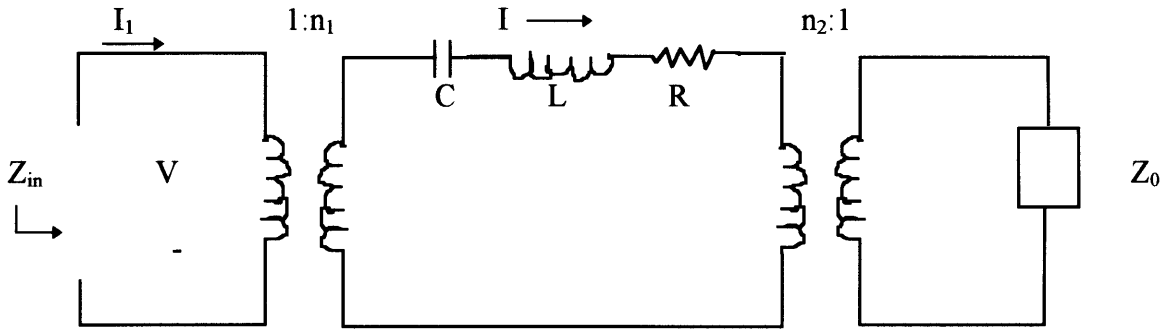

The impedance a measured by port 1 is then given by the following equivalent circuit:

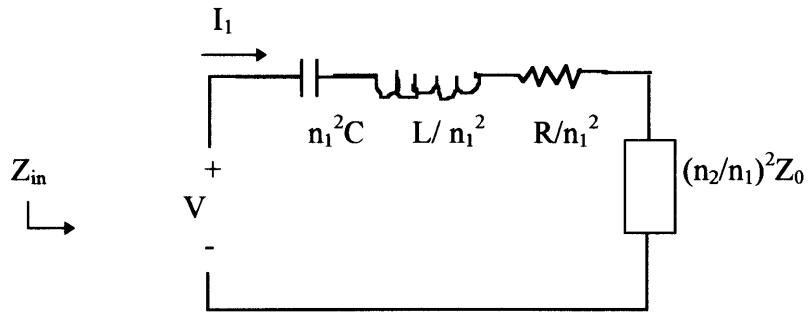

These two examples are quite useful for a variety of two-port measurements. Using these circuit models, it is possible to relate the measured impedance of a tag to its unloaded Q and also measure the amount of power being delivered to the tag. If the tag geometry and electromagnetic fields are known, then it is also possible to estimate the read range of the tag and calculate the currents and voltages within the tag.

F. Tag System Operation & Physical Limits

1. Frequency-domain vs. Time-domain

Once electromagnetic coupling to a tag is achieved, two basic detection schemes can be used: the incoming signal can be analyzed as a function of frequency or as a function of time. Of course, it is possible to perform a mixture of these as well. Both of these are ways in which the tag signal can be separated from that of the surrounding environment.

Frequency-domain detection is generally used for harmonic tags. The tag is excited at a single frequency, and then the resulting spectrum of the tag is measured. Frequency-domain methods are also used for resonant tags which contain resonators operating at more than one frequency.

Time-domain detection is commonly used for detecting resonant tags. Since resonators have the ability to store energy, they will continue to produce a signal after the excitation field has been turned off. Since most of the surrounding environment does not possess a significant Q, then the only signal which remains after the excitation pulse is the signal from resonators which operate at the excitation frequency (or a harmonic thereof). As a result, this "pulse-and-ringdown" approach provides an effective means of detecting small signals. For systems which operate over a small number of discrete frequencies, this method of detection can be quite cost effective.

2. Electromagnetic Shielding Effects

Electromagnetic shielding can occur when a foreign material is placed between the tag and the reader. If this material is electrically conductive or has ohm or dielectric loss, the tag signal will be attenuated, and in some cases, lost completely.

For inductively coupled tags, dynamic shielding is caused by eddy currents induced in the intervening material. (I assume the material does not have a high magnetic permeability, which would shield even a static magnetic field) According to Lenz's Law, these eddy current will produce a field to oppose the applied field, thus attenuating the desired signal. The time scale over which these eddy current last is a function of the dimensions and conductivity of the shielding material. The eddy current J resulting from the applied magnetic field H_a, is given by

$$\oint \frac{J}{\sigma} \bullet ds = -\frac{d}{dt} \iint_S \mu H_a \bullet da \qquad \text{(Eq. 54)}$$

This eddy current will in turn produce an opposing magnetic field, H_{op}, given by

$$\oint H_{op} \bullet ds = \iint_S J \bullet da \qquad \text{(Eq. 55)}$$

The shielding material thus behaves like a parallel L-R circuit: if a sudden field is applied to the L-R coil, then a voltage will be induced which will produce an opposing current and field. A smaller value of R will produce a larger current and will take longer to decay. Such a system is characterized by a time constant, τ=L/R.

If we think of a sheet of material as concentric annular rings with a similar L/R behavior, the time constant (known as *the magnetic diffusion time*) can be approximated as

$$\tau_m = \mu\sigma l_1 l_2 \qquad \text{(Eq. 56)}$$

where μ is the magnetic permeability, σ is the conductivity, and l_1 and l_2 are the transverse dimensions of the shielding material. If this diffusion time is long compared to the switching time of the applied field, then the applied field will be essentially shielded and the tag will not be detected.

For an electrically coupled tag, the shielding is produced simply by the rearrangement of the charge distribution within the shielding material. This displacement charge will produce an opposing field which will act to attenuate the applied electric field. The applied electric field induces a surface charge density given by

$$\rho_s = n \bullet \varepsilon E \qquad \text{(Eq. 57)}$$

Within a conducting medium, the unpaired charge will move according to the charge relaxation equation

$$\frac{\partial \rho}{\partial t} + \frac{\rho}{(\varepsilon/\sigma)} = -E \bullet \nabla\sigma + \frac{\sigma}{\varepsilon} E \bullet \nabla\varepsilon \qquad \text{(Eq. 58)}$$

By inspection, we see that the associated time constant (the electric relaxation time) is given by

$$\tau_e = \varepsilon / \sigma \qquad \text{(Eq. 59)}$$

It is desirable to have τ_e be long compared to the switching time of the applied field, so that the free charges in the shielding material will not have sufficient time to redistribute and produce an opposing field.

Since both electric and magnetic shielding effects are frequency dependent, we see that choosing an appropriate operating frequency is an important factor for a given application. In general, lower operating frequencies are best to minimize shielding; however, higher frequency systems have a faster response, which in RF-ID, also allows for a higher data rate. At present, a good compromise for commercial RF-ID tags is the 13.56 MHz ISM band.

For applications requiring relatively large electromagnetic fields (e.g. commercial or industrial applications requiring a long read range), electromagnetic shielding may be added on certain sides of the transmit antenna in order to reduce human exposure or to reduce electromagnetic emissions. In such cases is important to consider the effect of the shielding material on the electromagnetic field distribution. Magnetic shielding materials have a relatively square hysteresis loop and can also produce harmonics; therefore, in harmonic tag detection systems, precautions should be taken to minimize these spurious signals.

3. Read Range

For the consumer, perhaps the most important parameter of a tagging system is the reading distance. It is obvious that for the tag reader, we want to maximize the transmitter power and maximize the receiver sensitivity. Less obvious, however, is how the signal-to-noise ratio depends on the Q of the tag and the coupling.

For a tag to be read at a distance, three basic things are required:

1) The electromagnetic fields must couple sufficient power to the tag.

2) The tag must make efficient use of the energy in order to create a detectable signal.

3) The reader must be able to detect the signal perturbations produced by the tag.

For a materials tag, only the last two requirements are necessary. As a result, a materials tag can be made to function at longer distances than an RF-ID tag.

The estimated read range of a tag can be calculated using an appropriate circuit model such as the ones presented previously. A good estimate of the read range for an RF-ID tag can be derived simply from requirement #1 mentioned above. It is difficult to comment on the other requirements without discussing the particular details of the tag and reader electronic design. In most cases, the detection of a raw signal from an RF-ID tag is very similar to the problem of detecting a passive tag, such as a shop-lifting tag. The tag must have good detectability, either by having a high Q resonance or by being able to provide a modulated return signal at a frequency other than the excitation frequency. The basic issues for the reader are signal-to-noise ratio and the sensitivity of the receiver. However, unlike a shoplifting tag, RF-ID tag transmit time-varying digital data that must also be successfully interpreted. This issue involves many factors such as the modulation scheme used and the data protocols. Since these parameters vary significantly with manufacturer (at least until industry standards are enforced), it is perhaps most generally useful to discuss how the electromagnetic fields contribute to the read range. If the electromagnetic interactions are well understood, then the tag and reader design can be much better defined.

For a materials tag measured as a function of frequency, the signal detected at the reader is simply a function of the electromagnetic coupling and the impedance of the tag. The equivalent circuit models presented earlier show how the coupling and tag impedance can transformed into an equivalent impedance circuit. The electromagnetic coupling can be calculated from the geometry or measured in the laboratory using a vector network

analyzer and can be expressed in terms of the measured S-parameters and the loaded and unloaded Q. If necessary, impedance of the tag can also be measured at a known distance.

If the materials tag is being detected in the "time-domain" using a pulse and ringdown approach, then the problem must be divided into two separate steps:

1) Pulse phase: Calculate the amount of power transferred to the tag given an RF burst of a known duration.

2) Ringdown-phase: Modeling the tag as the source and the reader as the receiver, then calculate the amount of power transferred from the tag to the reader.

Each of these two steps will generally require a separate one-port circuit model. For the ringdown phase model it is necessary to know the input impedance of the reader (Z_{in}=50 Ohms is typical for lab instruments).

a) Tags with Loop Antennas

For an inductively-coupled RF-ID tag, the chip is powered mainly from the magnetically-induced voltage in the coil as given by

$$V = -\frac{\partial \Phi}{\partial t} = -\frac{\partial}{\partial t}\oint B \bullet dA \qquad \text{(Eq. 60)}$$

where B is the magnetic field produced by the reader coil, and the area A is the area contained by the tag coil. The dot product is used to calculate the orientation dependence of the pick-up voltage. From the time derivative, it is evident that the induced voltage increases linearly with frequency, which can also be calculated.

Of course, the pick-up voltage depends on the power of the reader; however, as in the case of a materials tag, the efficiency with which the power from the reader is transferred to the tag depends on the electromagnetic coupling and the impedance of the tag.

For an RF-ID tag, the maximum read range that can power the tag is determined by the impedance of the tag and the power requirements of the tag. Several types of diode rectifiers can be used on the chip to convert the AC pick-up voltage to the DC voltage necessary to power the remainder of the IC chip. The minimum operating voltage for CMOS is approximately 1 Volt, but the minimum required operating current depends greatly on the IC design (5-40 μA is typical). If the reader coil geometry and the electronic specifications of the tag chip is known, the maximum read range can then be calculated using the circuit models presented previously.

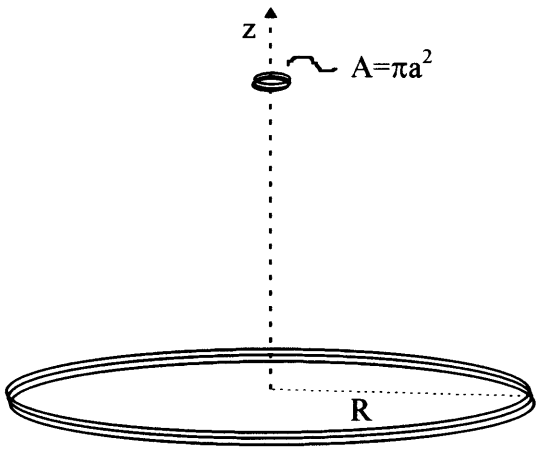

Figure 23. Example of tag and reader configuration used to estimate read range.

In the case shown in Figure 23, for example, the axial magnetic field produced by the reader is given by

$$B = \frac{\mu_0 I R^2}{2(z^2 + R^2)^{3/2}} = \frac{B_0 R^3}{(z^2 + R^2)^{3/2}} \qquad \text{(Eq. 61)}$$

where R is the radius of the reader coil, and $B_0 = B(x = 0) = \mu_0 I / 2R$. In this case, we can use the one-port mutual inductance transformer model, using the magnetic field distribution to calculate the mutual inductance. For a materials tag, or an RF-ID tag using a resonant antenna (coil + tuning capacitor), the power transferred from the reader is a function of the tag impedance and the electromagnetic coupling. However, using the circuit model, the coupled tag impedance can be transformed into the equivalent circuit impedance. Knowing the signal to noise ratio of the reader, and knowing the properties of the tag (e.g. Q, equivalent LRC, etc.), the read range as a function of the applied reader voltage can then be calculated.

b) Tags with Electrode Antennas

Tags which are electrically coupled can be analyzed in similar ways. The surface charge produced on the electrodes of a tag is given by

$$Q = \iint_S \nabla\varphi \bullet da \qquad \text{(Eq. 62)}$$

by gradient of potential dotted with surface. Current is then given by $i=dQ/dt$. The voltage across the tag is $V=iR$, where R is the tag resistance which can be measured.

For an RF-ID tag, we can assume a minimum voltage on the order of the CMOS voltage, which is at least 1.5V volt plus the amount of voltage drop across the internal rectifier. Given this estimate of the voltage, the read range is then determined by minimum current required for the chip to operate (20-40 μA is typical..

G. Tag Tracking

Since it is possible to relate the position and orientation of a tag to the measured signal, it is interesting to think about the possibility of predicting am unknown position and orientation of a tag from the measurement of its signal. Since this problem contains many degeneracies due to the inherent geometric symmetries, an array of receiving antennas would be required to extract the necessary information.

Chapter III.

Giving Birth to Information

Thousands of years ago, it is unlikely that somebody sat down one day and created from scratch hieroglyphics, or any form of written language that exists today. The written characters of language, Eastern or Western, have evolved – and presumably improved – over many years. Perhaps one day the same will be said for information encoded in electromagnetic signals.

Electromagnetic encoding is not new. Since the invention of Morse code, we have seen the invention of the telephone, radio, TV, and now many portable electronic communication devices, each introducing new flavors of information encoding. Perhaps the complexity of encoding static information in physical objects will follow a similar evolution.

A. Passive Tags as Bits

The information contained in a tag is not dynamically changing, unless the tag is functioning as a sensor and responding to local changes in its environment. As a result, we must stimulate the tag in various ways and then listen in time and frequency for the information. Perhaps some day it may be possible to efficiently interrogate a tag with an encoded sequence of pulses and wait for the tag to echo its response. We are not quite there yet.

1. Frequency Domain

Perhaps the simplest way of encoding information in a tag is to express the data in some digital form and then express the individual binary bits as an electromagnetic resonance. If the frequencies of the resonances are know beforehand, then by doing a frequency sweep, a digital "1" or "0" would be represented by the presence or absence of a resonance. This is illustrated in Figure 24.

The amount of information per tag which can be stored via this method is limited by the number of resonances that can exist per tag. Given N possible resonant frequencies per tag, it is possible to create up to 2^N-1 different tags. The primary factors which limit the number of resonances per tag are: the available bandwidth of the tag reader, the frequency resolution of the tag reader, the Q-factor of the resonances, and the physical size of the tag, and the desired read range. Discounting the possibility to store data in nuclear spin resonances, most types of resonators occupy a macroscopic amount of space, ranging from approximately 100 μm^2 to 100 cm^2 or so. For a tag reader of a given sensitivity, the read range generally scales with the size of the resonators in tag. For example, if a read range of 10 cm is desired, a reasonable corresponding resonator size would be approximately 2mm X 10mm, so this limits the number of bits in a credit card size tag to a few dozen, based on size alone.

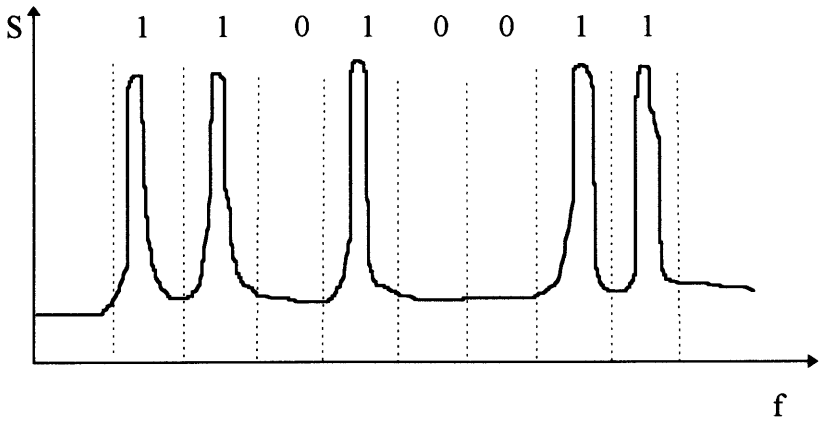

Figure 24. Sample response from a tag containing five resonators of different frequencies.

The resonators on a tag can also be coupled to each other in different ways in order to provide another degree of freedom for data encoding. Coupled resonators will beat together and give rise to harmonics and subharmonics. It is also possible to encode information in harmonic tags by creating harmonic tags with different harmonic spectra. Although this can be done through the shaping and processing of the harmonic material, this approach seems less reliable than the resonator approach.

2. Time Domain

Tags can be made to have differing transient responses. Naturally, the sub-harmonics generated by coupled resonators could also be observed in the time domain as an amplitude modulation on the existing frequencies. If frequency or phase can be viewed as

a function of time, it would also be possible to observe the evolution of energy modes among a given number of resonators.

For harmonic materials, the time domain could be used to encode information by sweeping the applied field sign and amplitude. By combining different pieces of harmonic material having different magnetization curves it may be possible to generate a rich set of amplitude-frequency sequences as the applied field is varied.

B. Passive Tags as Sensors

In addition to identification, a useful feature of electromagnetic tagging is in remote sensing of an object's state, such as temperature or pressure. In many cases, electromagnetic materials are well-suited for this purpose because it is possible to design structures which are sensitive to environmental parameters. Certain materials, popularly known as "smart materials," exhibit a direct coupling between their electromagnetic properties and other external stimuli such as pressure or optical excitation. Although sensor tags can be made from harmonic materials, encoding sensor data in resonator parameters is the most straightforward and is discussed below.

1. Encoding Data in F_o and Q

Sensor data can be most readily encoded in the Q-factor of a resonator by providing a means of degrading the Q via an external parameter. It is easier to increase energy losses than to reduce them, and the reciprocal of Q is proportional to the existing dissipative loss mechanisms in the resonator. However, because the *measured* Q also depends on losses external to the resonator, including the effect of antenna coupling, Q is an unreliable parameter for encoding information unless all external losses, coupling, and geometry are known. Certain sensor devices, such as accelerometers, contain mechanical resonators and may use Q as a sensor parameter; however, this fact does not imply that electromagnetically-coupled resonators can be used in the same way. The Q-factor of an electromagnetic resonator can be used to some degree, but for situations requiring more than 4 bits (i.e. 16 levels) of dynamic range, it is highly preferable to encode the sensor information in the resonant frequency of the resonator. Also, from the perspective of the tag reader function, it is much easier and more accurate to measure frequency than Q.

2. Examples

a) Force Sensor

Most force sensors on the market today function as variable resistors, whose electrical resistance is a function of the applied force or pressure. Unfortunately, the response of these devices is relatively noisy and hysteretic. Much of this is due to the fact that these devices no not rely on an intrinsic microscopic property of the sensor material, but instead rely on an average macroscopic response of the sensor structure. A typical resistive force sensor makes use of the effective resistance of the sensor structure, which can be comprised of conducting particles in a semi-insulating matrix, or layers of conducting cilia-like structures. As these structures are compressed, their resistance decreases due to decreased percolation threshold (in the particle case) or increased connectivity (in the cilia case). Because the effective resistance of these structures is an average of a finite number of discrete distributed conducting pathways, their resistance is not a smooth function of the applied force. This is particularly noticeable when trying to resolve small changes (e.g. $\leq$ 5%)in the applied force. As one might expect, it is also difficult to make a very thin ($<$ 1mm) force sensor of this type which has good resolution as well as a high dynamic range (e.g. .01-10 Newtons).

In order to demonstrate the use of a electromagnetic resonator as a wireless force sensor, a planar LC resonator was fabricated, using a force-sensitive dielectric. Although the obvious approach might be to insert a rubber-like foam between the capacitor places, we wanted to make the sensor as thin as possible, so a piezoelectric polymer was used as the dielectric. The two-coil planar resonator was designed and etched from copper clad 1000K120 Kapton made by Rogers. The two coils were then folded upon each other, with a 25mm dielectric placed between the two layers. The dielectric region was comprised of either teflon sheet or the piezoelectric polymer polyvinyldifluoride (PVDF), supplied by AMP, Inc. The structure was then epoxied under vacuum or laminated to seal the dielectric between the layers.

The performance of the sensor tag was evaluated using an Instron 4411 mechanical tester and the HP network analyzer (see Figure 25). The sensor tag was placed over a 2" diameter sapphire base containing a loop antenna. The whole assembly was placed onto the lower anvil of an Instron machine. On top of the coil assembly, a 3" x 3" x 3" cube of non-conducting foam was placed between the sensor tag and the top anvil. Both the network analyzer and Instron press were connected to a PC via a GPIB interface. The Instron was programmed to apply a load in increments and output both the applied load and displacement from the origin. The resonant frequency and Q-factor for of the sensor tag was simultaneously recorded. These numbers form the basis for the data. The specific force sensor demonstrated in this paper is designed to have a sensing range similar to a human finger, so an applied load range of 0-5 Newtons was chosen.

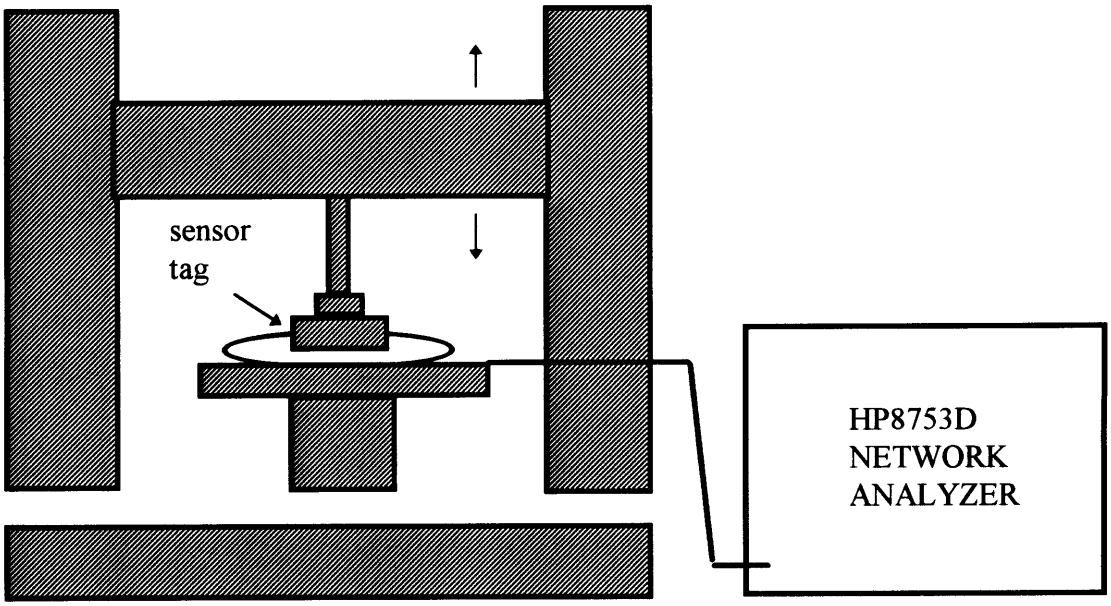

Figure 25. Schematic diagram of the test apparatus for testing the force sensor.

The resonant frequency response of the planar tank circuits with PVDF dielectric was compared to that of tags containing Teflon, a conventional high-frequency dielectric. Results are plotted in Fig 26.

For the resonator containing the normal dielectric, its response can be modeled as a simple LRC-circuit composed of an inductor, resistor, and plate capacitor with a dielectric material. By applying an elastic model to the deformation of the dielectric material under applied stress, the resonant frequency of the tag can be derived as a function of applied stress:

$$\omega_n = \omega_{n_0} \cdot \sqrt{\frac{E-\sigma}{E}} \qquad \text{(Eq. 63)}$$

where ω_{n_0} is the resonant frequency of the tag absent any applied stress, E is the Young's Modulus of the dielectric material, and σ is the applied stress. Rearranging Eq. 63 yields an expression relating the ratio of the change of resonant frequency versus initial resonant frequency and the induced strain, ε, in the dielectric material:

$$\frac{\Delta\omega}{\omega_{n_0}} = 1-\sqrt{1-\varepsilon} \qquad \text{(Eq. 64)}$$

The measured data and the curve predicted by this model is included in Figure 26 and very closely matched the measured data to within 0.1%.

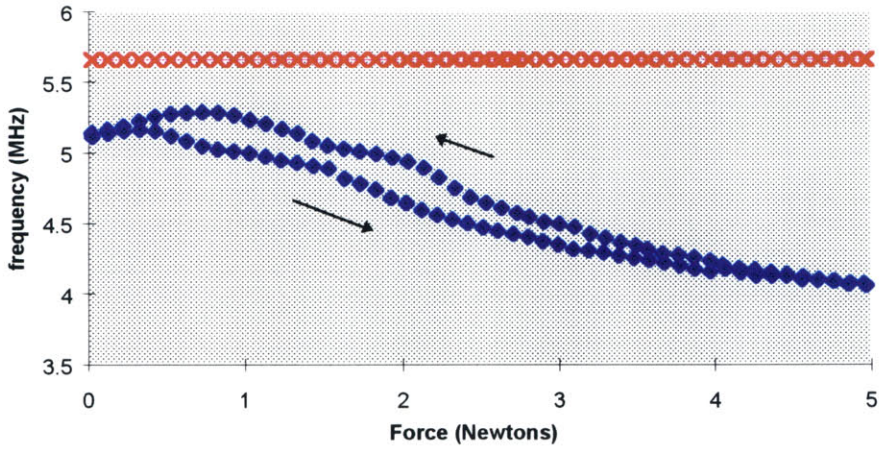

Figure 26. Data for wireless force sensor incorporating a piezoelectric polymer dielectric (lower curve). The upper curve is the response of an identical resonant structure incorporating a normal dielectric material (teflon). Superimposed on the upper curve is the predicted curve derived from the linear elastic model.

In comparing the teflon response to the response produced using PVDF, this model indicates that in a typical dielectric material with Young's Modulus of about 3 GPa (comparable to PVDF and clear teflon sheet), a 10% change in frequency would occur when there is a strain of 19%. Further manipulation of equation (2) shows that in order to produce in a 10% change in the resonant frequency of the tag, a force of 60000 Newtons would need to be applied to the tag. On the other hand, the tag incorporating the piezoelectric material shows a significant response with an applied force of as little as 0.1 Newtons. A theoretical curve (not including hysteresis) could be derived for the piezoelectric response by solving the coupled tensor equations:

$$\begin{aligned} \varepsilon E &= \varepsilon_T E + dT \\ S &= dE + s^E T \end{aligned} \qquad \text{(Eq.65)}$$

where, E is the electric field, T is the mechanical stress, d is the piezoelectric coefficient, ε is the complex permittivity at zero stress, and s^E is the mechanical compliance at zero field.

The primary advantages of the PVDF force sensor tag are its small thickness (< 0.5 mm) and good sensitivity to small forces. The main apparent disadvantage of this sensor is hysteresis. Piezoelectric materials are intrinsically hysteretic, but their response is repeatable. Some hysteresis, however, can be partially attributed to the packaging of the PVDF and thus can be improved with better packaging design. This type of sensor has also proven to be quite robust, and continued to perform with no noticeable degradation in sensitivity even after subjecting this force sensor to abuse, such as stepping on it or striking it with a hammer. We also estimate that the manufacturing cost of such a sensor could be less than $0.05.

b) Humidity Sensor

Another interesting structure that can be made from a planar LC resonator and piezoelectric polymer is a humidity sensor. The test design for this structure consisted of a single planar coil with connection to an opposing electrode forming the opposite plate of the capacitor. The piezoelectric polymer between the capacitor plates was sized to protrude slightly from the edges of the capacitor and exposed to the ambient environment. A rigid substrate was used for the sensor to avoid piezoelectric effects due to flexure. A simple sketch of the structure is shown in Figure 27.

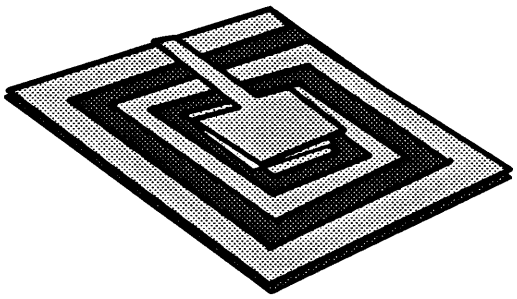

Figure 27. Sketch of the humidity sensor, showing planar LC resonator with piezoelectric polymer dielectric.

Quantitative evaluation of this sensor has yet not been completed, but the empirical results look very promising. Breathing on the sensor produces a positive frequency shift on the order of 10% and the sensor response appears smooth and repeatable. If a hand is held over the sensor, the sensor exhibits a frequency shift of several percent simply from the humidity emanating from the palm of the hand. It was originally thought that the sensor response was thermally activated, but upon further evaluation using a variable temperature chamber, hot plate, and application of different gas environments (dry helium vs. humid air), the sensor exhibited no thermally-induced frequency shift greater than the expected shift from thermal expansion. It is currently suspected that the humidity induced frequency shift is due to a surface charge effect at the edge of the capacitor which produces a humidity-dependent leakage across the plates thus reducing the effective capacitance. The observed 10% frequency shift corresponds to a 20% change in the capacitance and is consistent with this explanation given the dimension of the capacitor plates and the theoretical contribution of the edges to the capacitance

$$C = \frac{\varepsilon A}{d}\left[1 + \frac{\ln(\pi a / d)}{\pi a / d} + \frac{\ln(\pi b / d)}{\pi b / d}\right] \qquad \text{(Eq.66)}$$

where a and b are the transverse dimensions of the plates, and d is the spacing between the plates.

c) Linear Position Sensor

It is currently a challenge to wirelessly measure the linear position of a piston within a cylinder. In manufacturing applications, currently technology consisting of a magnet and hall sensor cannot measure continuous position but only detects when the piston has reached a certain position. As a possible solution to this problem, we designed a simple displacement sensor using a magneto-mechanical resonator for the purpose of measuring the linear position of a piston in a small cylinder (10cm long). A strip of amorphous metal ribbon packaged in a plastic cavity was attached to the body of the cylinder. Additionally, a weak flat bias magnet made of Arnochrome 3 ^{TM} of ~ .5 Oe or so can be included with the ribbon to provide a small constant bias field; however, for simplicity this additional magnet was not used for this study. The magnetoelastic ribbons used were amorphous alloys manufactured by Allied Signal and prepared in a width of 1.2cm and length of 3.55 cm. A properly oriented permanent magnet was attached to the end of the piston, thus providing a bias field to the ribbon which varied with linear position of the piston but did not vary with azimuthal rotation of the piston shaft (Figure 28).

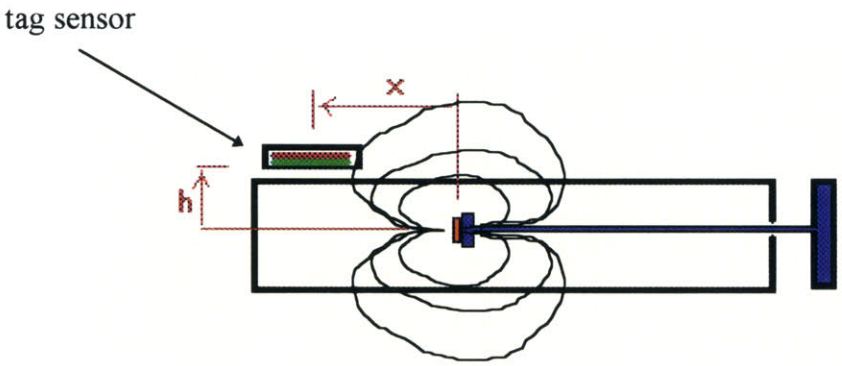

Figure 28. Schematic view of cylinder with position sensor, showing the magnetic field lines emanating from the permanent magnet mounted on the end of the moveable piston.

Since the resonant behavior or the ribbon depends on the bias field as well as its material properties, the linear position of the piston could then be deduced by tracking the resonant frequency of the ribbon. The basic conceptual approach is illustrated in Figure 29. The dependence of the local bias magnetic field presented to tag as a function of piston position could be varied by changing the mounting position of the tag on the cylinder; and the resulting resonant frequency shift resulting from this field could be also be tuned independently through annealing treatments of the amorphous metal ribbon.

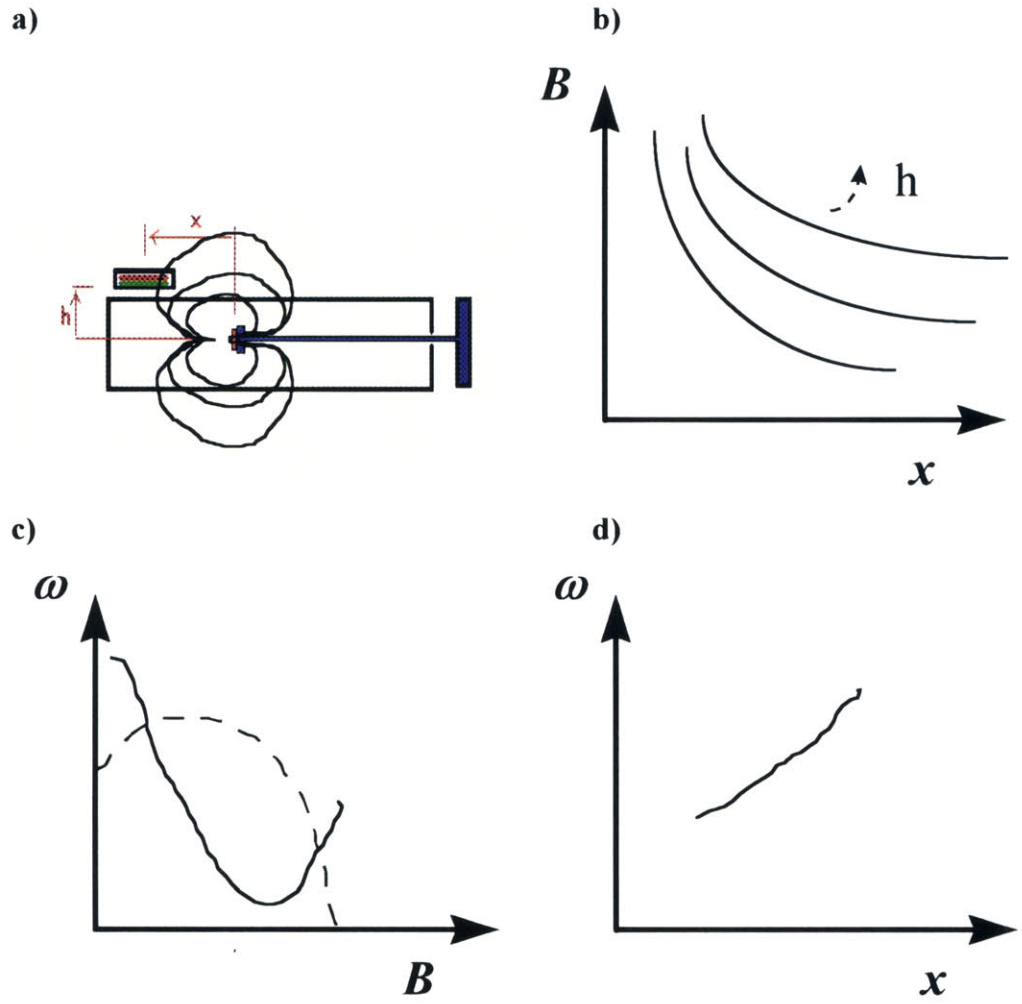

Figure 29. Illustration showing the basic concept of the position sensor. a) illustration of cylinder configuration (same as Figure 28) b) the magnet field measured at the position of the sensor as a function of the linear position of the piston. c) data showing how the sensor frequency (solid line) and amplitude (dotted line) vary as a function of the applied magnetic field. d) sample data showing how the resonant frequency of the sensor varies as a function of the piston position.

In order to increase the linear distance over which the sensor could operate, a preliminary annealing study was carried out to investigate the optimum processing parameters for the ribbons that were tailored to this application. Since it was desirable to increase the usable range of bias fields, a slightly sheared M-H loop is desirable, so a transverse-field anneal was used. Samples of composition $Fe_{38}Ni_{39}Mo_{2.4}B_1Si_{0.2}$ were annealed at a temperature near 400 degrees Celsius using several different annealing fields. A second alloy used for this study was $Fe_{35}Ni_{33}Co_{19}B_8Si_5$, which was annealed by Sensormatic using another recipe. The resonant frequency shift as a function of an applied DC bias field was then measured using an Hewlett-Packard 8753D Network Analyzer. A representative sample of the measured data is shown in Figure 30. For

$Fe_{38}Ni_{39}Mo_{2.4}B_1Si_{0.2}$, we suspect the annealing temperature was slightly higher than optimum, as exhibited by the extra degree of flattening in the curves likely due to partial recrystallization of the amorphous metal.

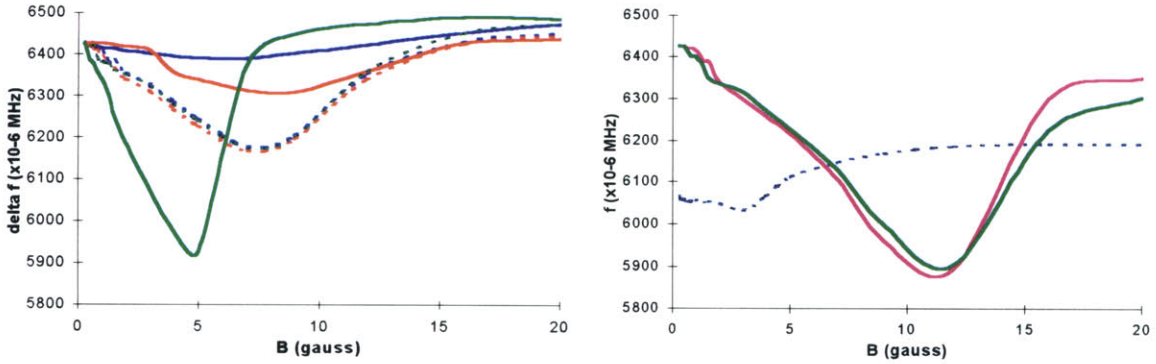

Figure 30. Bias-field dependence of the resonant frequency as a function of annealing treatment. On the left is data for $Fe_{38}Ni_{39}Mo_{2.4}B_1Si_{0.2}$ for transverse annealing fields of 0, 200, 300 Oe. (curves for higher fields are flatter) On the right, is the result for $Fe_{35}Ni_{33}Co_{19}B_8Si_5$ after the Sensormatic annealing treatment. Dotted lines denote pre-annealed as-cast result.

One sample of each type of amorphous metal sample was selected for use as the sensor tag and mounted on the cylinder. The resonant frequency of each tag was then recorded as a function of the piston position. The results are shown in Figure 31.

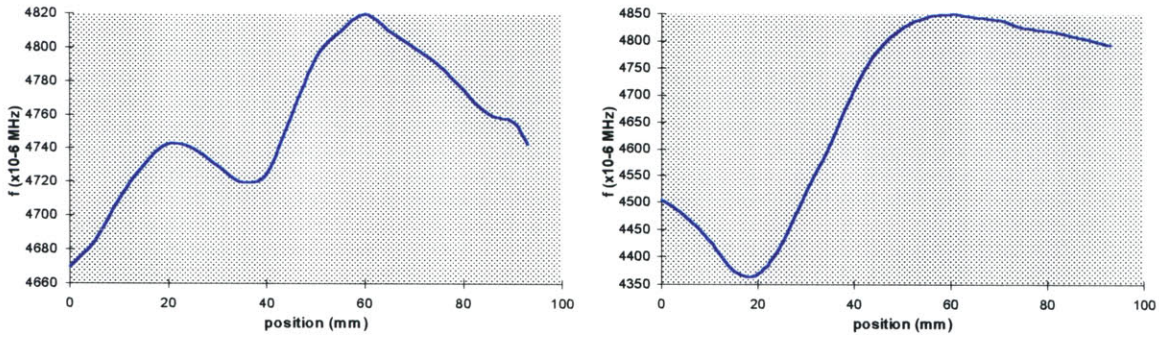

Figure 31. Plot of tag frequency vs. piston position for $Fe_{38}Ni_{39}Mo_{2.4}B_1Si_{0.2}$ (left) and $Fe_{35}Ni_{33}Co_{19}B_8Si_5$ (right).

As shown in Figure 31, the usable sensing range was approximately 2 cm (from x = 40 mm to x = 60 mm) for $Fe_{38}Ni_{39}Mo_{2.4}B_1Si_{0.2}$, and was approximately 4 cm (from x = 20 mm to x = 60 mm) for $Fe_{35}Ni_{33}Co_{19}B_8Si_5$. By further optimizing the placement of the sensor tag as well as the strength of the permanent magnet used, it should be possible to extend the usable range of operation to 8 cm or more for a cylinder of this size (10 cm long). For a larger size cylinder, the design can be scaled up using a larger size magnetoelastic ribbon; or for very long cylinders, separate tags can be used along the length of the cylinder to track the piston position along the entire length of its stroke.

C. Passive Tags with Memory

If it were possible to induce a stable change in a material's state over some distance, then it would be possible to reversibly change the information contained in a material tag. The ability to reprogram the information in a tag is a powerful feature which would enable objects to have memory and would allow us to know the history of an object. This would allow us to store information on a package or a book binding in a manner very analogous to the way information is written on credit cards or ATM cards now. Of course, the advantage of an electromagnetic tag is that the information could be written and read from a distance.

1. Current Technology

At present, there exist 1-bit writeable tags, which means the tag has only two states, ON or OFF. This class of tags is commonly used as shoplifting tags in the EAS (Electronic Article Surveillance) market. In the EAS industry, changing the state of a tag from the armed state to the unarmed state is known as *tag deactivation*.

For a harmonic type of tag (described previously), tag deactivation is done by adding to the tag a strip of semi-hard magnetic material, such as Arnokrome-3, which adds a bias field which serves to shift the M vs. H curve of the harmonic material outside of the range of the excitation field. Assuming, for example, that the non-linear "step-portion" of the magnetization curve occurs exactly at the origin, then if the added bias field is larger than the maximum amplitude of the externally applied excitation field, then the excitation field will never be able to flip the magnetization of the harmonic material. As a result, the tag will remain in one of its saturated magnetic states and thus produce no flux jumps and no harmonics. However, if the bias magnet is demagnetized, then the magnetization curve will once again be centered at the origin and the tag is once again operational (i.e. ON).

In the case of a resonator type of tag, deactivation in LC resonator tags is generally carried out by applying a strong magnetic field pulse which shorts out either the capacitor or shorts out the turns in the inductor. In both these cases, these "weak links" are purposely designed into the tag and are not a general characteristic of LC resonators. For a magnetomechanical resonator, the tag can be deactivated by demagnetizing the bias magnet packaged with the tag, thus disabling the magneto-mechanical coupling which allows the tag to vibrate. Unlike the case of the LC resonator, deactivation of a magnetoelastic tag is not destructive, so the process is reversible.

It should be noted that all the reversible mechanisms mentioned here rely on magnetizing or demagnetizing a strip of material. Due to practical considerations (available power, safety issues, etc.), these approaches are limited to a distance of 10 centimeters or so.

2. Possible Approaches

A desirable goal for writeable electromagnetic tags is to be able to individually address bits within a tag over a fair distance (.1m or more). Approaches we are investigating include frequency-addressed and field-addressed bistable mechanisms. Bistable material mechanisms is needed in order to maintain a stable change in state, and frequency- and field- addressing schemes can be used to provide bit selectivity. Certainly, energy considerations are perhaps the greatest constraint in trying to achieve operation over distance. To this aim, resonators could be useful, since they not only provide frequency selectivity, but they also serve as a means of storing and effectively amplifying available energy.

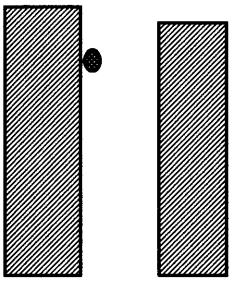

Figure 32. Sketch outlining the principle of a bistable frequency addressed read-write tag. Shown are two separate frequency resonators with a small magnetic exchange particle.

Work in this area is ongoing, so I shall only present an illustration of a frequency addressing concept using a mechanical analogy. Consider the tag in Figure 32, which contains two magnetoelastic ribbons, each cut to a different length thus having different resonant frequencies. It is assumed that a sufficient bias field is present so the strips can function as magnetomechanical resonators. In addition there is a small magnetized particle which can attach itself to either strip. When the particle attaches itself to a strip it increases the total resonator mass, thus lowering its resonant frequency; this means that there are four distinct frequencies which can exist on this tag. In addition, if a strip containing the magnetic particle is excited, then the resulting vibration can be enough to cause the particle to detach itself from that strip and attach itself to the other strip. Given this information, it is theoretically possible to fabricate a multi-bit writeable tag that could operate over a reasonable distance (> .1m), with each bit consisting of two resonators and four operating frequencies (2 for reading, 2 for writing), for example. In practice a similar mechanical approach I tested in the lab did not prove sufficiently robust for practical application, but I am pursuing other non-mechanical bistable mechanisms.

CHAPTER IV.

Implementing Materials Tag Technology

The preceding chapters described the operation of various types of electromagnetic tags. Obviously, the goal of our research is to incorporate materials tags into a variety of electronic systems and commercial devices. This chapter describes a practical tag reader system and gives some examples of commercial applications.

A. A Practical Portable Tag Reader

Although much of this document is devoted to discussing the design of the tag itself (which has been the main focus of my research), obviously a crucial element necessary for implementing this technology is the tag reader. In the laboratory, various types of vector or scalar network analyzers and other instrumentation can be used to carefully analyze and measure tag signals. However, such instrumentation is quite expensive (>$50,000), large, and heavy. Certainly, a commercial tagging system should include a tag reader that is relatively low-cost and preferably portable.

In the following sections, I describe my design for a general purpose tag reader which illustrates the basic functions required. The tag reader hardware can be divided into two main parts, the electronics and the antenna(s). The tag reader described below uses inductive coupling and can be used to sense both magnetoelastic tags and harmonic tags. Also, it can be built using less than $100 in parts. I have chosen to name the tag reader box the Mpulse unit and the antenna assembly the Senso-rings.

1. The M-pulse Unit

A block diagram of the Mpulse unit is given in Figure 33. This circuit uses two PLL (Phase-Locked Loop) -based frequency synthesizers. One synthesizer is used to generate the transmit frequency, and the other is used to generate the detection frequency, which is needed to look at the harmonics. The two PLL's can share the same crystal source, so that the two generated frequencies will have a set phase difference. The divide-by-N counter chosen was from the Motorola MC145157 which allows for 14-bits of frequency resolution, which is necessary in order to maximize the operating frequency range but also permit detection of narrowband features, such as a typical .1KHz-wide resonance peak. Both frequency synthesizers can be controlled using a small cheap microcontroller, such as the Microchip PIC16C71.

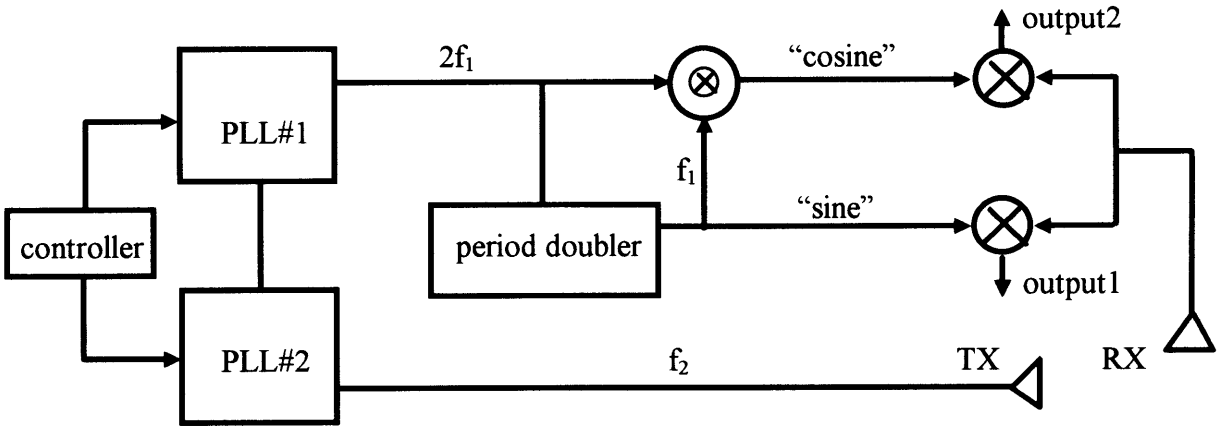

Figure 33. Block diagram of a simple tag reader which can be used to detect both resonant tags and harmonic tags. The excitation frequency is f2 and the receive frequency is f1.

Since the receive signal can possess arbitrary phase shifts due to the tag and the surrounding environment, it is desirable to detect both amplitude and phase of the tag signal. Since the operating frequencies are within the range of digital clock speed, I decided to produce the necessary in-phase and out-of-phase detection signals digitally in logic, rather than using an analog 90° phase shifter, for example. Given a square wave B, and a signal at half the frequency (generated using a period doubler), the gate A XOR B produces an output which is 90° out of phase with signal A. Some additional amount of buffering may be necessary to eliminate possible timing glitches due to the unequal component propagation delays. However, this avoids the problem of having to design an analog phase shifter network which can maintain a constant phase shift over a wide range of frequencies.

Both the receive signal and a given detection frequency signal are fed into a synchronous demodulator whose analog output is then fed into an A/D converter. The 8-bit A/D converters in the PIC 16C71 are sufficient for short range signals. However, if the tag reader is intended to operate over a wide range of distances or if it will be used to

track a tag's position from signal strength, then a logarithmic amplifier and an external 12 or 14-bit A/D converter is recommended.

2. The Senso-Rings

A crucial part of a tag reader system is the near-field antenna design. Unlike electrostatic coupling, inductive coupling offers particular challenges due to the relatively large drive currents involved and the inductance of the coils. In order to maximize the tag read range, it is desirable to maximize the excitation field and thus maximize the current in the antenna coil (of course, the antenna needs to be large enough to provide sufficient mutual inductance between the coil and tag). While the magnitude of the magnetic field is proportional to the number of turns in the coil, the inductance of the coil increases as the square of the number of turns, so it is best to increase the current in the coil rather than the number of turns. A high inductance load is undesirable for the circuitry which drives the coil because it creates a large amount of reflected power (back EMF) and presents an impedance which varies significantly as a function of frequency. In order to make a transmit coil which can be driven with a moderate amount of voltage (<30V), it is usually desirable to add a series resistance to the coil and only use a moderate number of turns (the number depends on the diameter of the coil). It should also be noted that the transmit coil should not be made to resonant as means of increasing its output power. Any resonance in the coils (transmit or receive) will provide a highly non-linear coupling as a function of frequency, which will make it very difficult to do a background subtraction or calibration of the tag reader, and will also reduce the amount of detection dynamic range that can be devoted to the tag signal.

For the receive antenna, it is desirable to maximize the number of turns in the coil in order to maximize the amount of EMF induced in the coil by the changing magnetization of the tag. However, the number of turns should be kept low enough so that the self-resonant frequency of the coil lies significantly beyond (above) the maximum operating frequency of the system. The self-resonance of the coil can be measured by exciting the coil with an RF burst and then observing its ringdown. This resonance is due to parasitic capacitance, and can be minimized by adding some spacing between the turns in the coil.

B. Sample Applications

As introduced in Chapter 1, the ability to sense and identify objects and people in the local environment is a need that will naturally increase as computers and automation grow more advanced. The following examples are mostly near-term applications that serve to illustrate basic commercial markets where low-cost electromagnetic tagging can have an impact.

1. Access: Ticket Tags

Electromagnetic tagging in the form of RF-ID is already being used in ID badges for access to buildings and offices; inside a building this badge can be used to customize a person's environment, allowing for example, computers to identify a person and automatically log them in or to track a person's location to send them messages. However, in the case of entertainment venues, such as a theme park or a dance club, a customized environment may be desirable, but it is simply too expensive to give all customers an RF-ID badge with their ticket.

Materials tags would increase the market for location-based entertainment by allowing entertainment companies or club owners with a cheap way of customizing a visitor's experience. A materials tag embedded in an admission ticket need not identify a person in terms of name, phone number, etc., but it can include basic information, such as age range (over 21 or not), male or female, and what language you speak, so that the rides, displays, and experiences inside the park or club can be customized. The admission tickets can also contain sensor tags (e.g. pressure) either to sense a visitor's emotional state (e.g. excited or not) or to be used as an control input allowing the visitor to interact with the entertainment in some way.

2. Packaging: Electromagnetic Barcode

Although a materials tag that costs 3¢ may be more expensive than an optical barcode (printing cost), it has many advantages which can add great value. An electromagnetic barcode would allow objects to be identified in applications where a scanning laser is not desirable. Also, since a materials tag reader does not need optical access, it can be hidden behind a panel and used in dirty or cluttered environments. A materials tag can be read in a variety of orientations and is also potentially reconfigurable. These advantages allow for greater automation, portability, and increased efficiency in "scanning-in" objects.

3. Industrial Processing and Manufacturing: Wireless Sensors

Certainly, manufacturing technology is very important to all industrialized nations. Adding sensors can provide new types of automation which can increase both the throughput and quality of manufactured parts. Materials tags can provide a low-cost method of identifying parts flowing down an assembly line, but perhaps a greater innovation would be the use of tags as sensors.

Modern day manufacturing plants are full of wires. Materials tags would not only provide alternative ways to incorporate low-cost sensing, but would also help to reduce the amount of wiring in factories. Wireless sensing would enable sensors to be incorporated into systems in which sensors could not otherwise exist. Additionally, since such sensors could be made from robust or high-temperature materials, it would be

possible to integrate sensors into certain hostile environments where silicon-based sensors could not operate.

4. Computer Interfaces: Smart Objects

The revolution in computers has been quietly deceptive. Deceptive, because the external appearance of computers has changed little over the past two decades. But inside the computer case, the amount of computational power and information storage has increased by orders of magnitude. Computers are also now networked together, and most of the traffic on telephone lines around the world no longer contain human voices but rather computer data. So much information now exists inside computers and flows in the unseen world communication networks, that it has defined a *digital* world.

Most of the research in information technology can be summarized as an effort to find better ways to interact with the digital world. Machines are not human, but we have been developing software which allows computers to adapt to human expectations and desires. At present, computers can see out into the physical world only by using a video camera, and we can see into the digital world only by looking into the monitor; audio information flows through the speakers and microphone; and printed information flowing in and out of the digital world is confined to the monitor, keyboard, printers and scanners. But regardless of how great these peripherals may be, they cannot yet identify people and object from their image or their sound alone. In addition, since digital information is not expressed in any physically tangible manner, we cannot manipulate digital information objects as easily as objects in the physical world. As a result, we still remain quite isolated from the digital world.

Electromagnetic tagging technology provides new connections between digital and physical worlds. At the expense of embedding tags into objects, it allows computers to sense and identify objects around them. Electromagnetic tagging compliments computer vision technology since it does not require line-of-sight and does not require a controlled visual environment. Sensor tags provide the ability to probe various properties of the physical environment (temperature, light, pressure, etc.) and provides new input alternatives to the keyboard and mouse. Combined with active material structures, tags also help to provide ways for computers to express their information by altering the state of objects in the physical environment. The ability to interact more naturally with computers by manipulating and observing tangible objects on a desktop or around a room, has dramatically changed our perception of a *human-computer interface*. At the MIT Media Lab, research in this area is being done by the Tangible Media Group, led by Prof. Hiroshi Ishii.

CHAPTER V.

Final Comments

This document was intended to serve as a brief but comprehensive introduction to near-field electromagnetic tagging as well as presenting some research results. My thesis work has included performing a survey of all the common forms of electromagnetic tagging that exist and developing a unifying description of the field. This has also included sketching out a theoretical framework which can be used to model all types of electromagnetic tags. In my relationships with many commercial sponsors, I have tried to identify certain key applications (at least the ones I am allowed to mention here) and in my lab work I have designed and created new types of electromagnetic tags to address some of these needs (mostly sensor needs). This work is ongoing.

In this closing chapter, I thought it would be useful to identify areas of ongoing work at the MIT Media Lab and also insert some personal opinions about the future of electromagnetic tagging.

A. Present Challenges and Ongoing Work

In order to make passive materials tags a widespread technology, further research is needed in three key areas: *efficient data encoding*, *multiple-object detection*, and *data-write capability*. Significant progress in any one of these areas would have a great impact in the commercial market. All of these require work at all levels of description, ranging from basic materials characterization and electromagnetic calculations to manufacturing considerations and tag reader design. Ongoing work at the MIT Media Lab addresses these issues and are discussed briefly below:

1. Efficient Data Encoding

For ID applications, a large number of data bits is desirable (e.g. 32 or more). With materials tags, it is most straightforward to encode data in the frequency domain. As discussed previously, limitations in the tag and in the reader limit the available frequency span and the achievable bit density. Current research involves exploring time-dependent materials phenomenon for encoding data as well as devising the appropriate coding algorithms which would make efficient use of the time-frequency code-space. If we think of materials tags as the physical analog of data hiding, I think there will be an increasing need among manufacturers to hide data in physical objects.

In order to minimize the physical size of a tag, we are currently exploring coding methods which make use of harmonic tag materials such as amorphous alloy wires. Compared to magnetoelastic ribbons, amorphous alloy wires do not need to be free to vibrate and thus can be easily woven or embedded into structures. In addition, harmonic tags can be operated at relatively low frequencies (<1 KHz) which are less easily shielded in lossy media.

2. Multiple-Object Detection

One of the most sought-after goals in all types of tagging technology is to find ways to identify many objects simultaneously. In the retail market, for example, such technology may allow supermarket customers to push a cart full of groceries through the check-out counter all at once, instead of requiring a cashier person to scan in each object one-at-a-time. A similar benefit also exists for security applications.

In both RF-ID and passive tag technology, the two main difficulties in detecting multiple objects are: tag antenna detuning, and time-frequency data collisions. If several tags are placed in close proximity to each other (overlapping) the combined mutual inductances act to detune the individual tag antennas. Additionally, if the information in the tags happen to share any portion of the time-frequency data space, then the tag reader will have difficulty discriminating between them.

A solution to the problem of multiple-tag detection now exists in some RF-ID technology. This solution makes use of a very powerful feature of RF-ID: *programmability*. In one approach, for example, the program in the RF-ID chip allows the reader to selectively deactivate a tag once its code has been read. By programming the tags to respond at pseudo-random time intervals, such a scheme permits the tag reader to read one tag at a time until all tags have been read. It is interesting to note that this approach will work even with many tags having identical ID codes. The basic scheme is outlined below.

EXAMPLE: Reader and 2 tags, A and B

Step 1: Reader sends interrogation signal
Step 2: Tag A and Tag B respond simultaneously
Step 3: ID Signal is not recognized
Step 4: Reader sends interrogation signal
Step 5: Tag B responds first
Step 6: ID signal is accepted
Step 7: Reader sends unique acknowledge code which deactivates tag B
Step 8: Reader sends interrogation signal
Step 9: Tag A responds
Step 10: ID signal is accepted
Step 11: Reader sends unique acknowledge code which deactivates tag A
Step 12: Reader sends interrogation signal
Step 13: no response
Step 14: Reading process completed

In materials tags, it is possible to read multiple tags if the tags do not contain overlapping frequencies. However, if we are able to control the transient response of material structures then we may be able to differentiate tags using time as well as frequency. As illustrated in the example above, a mechanism for remotely changing the state (e.g. deactivation) of a particular tag would also be useful.

3. Data-Write Capability

As mentioned in chapter 3, there is an interest in developing multi-bit writeable tags which can be read as well as written from a reasonable distance (>.1m). Compared to other types of tags, this is a longer-term project. The approach we are using is the development of tags using frequency-addressed and field-addressed bistable material mechanisms.

Being able to remotely reprogram the state of a material begs the question of being able to use a material to perform some sort of computation on the information is it given. For this reason, it is worth mentioning that our group, led by Neil Gershenfeld, is also very much involved in a project to do just that. It has been shown [reference] that is possible to use nuclear spins to do computation in materials through clever application of magnetic field pulse sequences. Perhaps out of this work in quantum computation in materials we will see a way to do better manipulation of states in a material tag structure through the clever application of pulse sequences.

4. Electromagnetics

Part of the ongoing work in tag technology includes includes applying simple electromagnetic models in order to predict and quantify tag performance. An obvious need for electromagnetics is in using antenna arrays to track the position and orientation

of tags in space. Electromangetic calculations and measurements are also needed to determine parameter values, such as the electromagnetic coupling, for use in tagging system equivalent circuit models sketched out in Chapter 2.

Another electromagnetics issue is the fact that the signal produced by electromagnetic tags is not isotropic. At the very least, this is due to the fact that tags are not shaped spherically symmetric. In addition, the tag reader antennas are either electric or magnetic dipoles which are themselves orientation-dependent. Although we are interested in exploiting the spatial dependence of the signal as a means of tracking the position and orientation of a tag in space, sometimes this property is undesirable. Materials tags are much less orientation-dependent than a barcode, for example, and can be made completely orientation-independent by using three orthogonal antennas, but we want to explore various alternatives. Part of our work includes experimentation with different tag shapes and antenna geometries.

B. Passive Tags vs. RF-ID

The preceding chapters have laid out the basic theory and application of passive materials tags. It is worth noting, however, that much of the engineering theory presented also applies to RF-ID tags, which were introduced in Chapter 1. For the benefit of people reading this thesis who would like to apply electromagnetic tagging to a particular application, it is worth describing the relative merits of both these technologies.

If we consider a midrange RF-ID tag (~$1.10 wholesale) and a midrange materials tag (~$.04, wholesale price of a current resonator type shoplifting tag), it is evident that RF-ID tags are considerably more expensive. However, the added cost provides the benefit of the digital chip, which can provide greater functionality. For example, the digital logic can be programmed to respond only to a particular digital interrogation sequence from the reader. Certainly, one advantage of RF-ID tags over passive materials tags are their ability to carry a large number of ID bits (32 or more) within a relatively compact package (~2cm X 2cm X 2mm, for example). Perhaps most importantly, RF-ID tags can be made to contain programmable memory (usually a few bytes) which can be written remotely from the reader. The use of the electronic chip, however, requires a certain minimum amount of power which thus reduces the read range in RF-ID devices. A quantitative analysis of the power budget and resulting read range for an RF-ID chip is currently being developed at the Media Lab.

Passive materials tags have the advantage of lower cost, but also posses other less-obvious advantages. A passive materials tag can be easily adapted to perform sensing of the local environment; this feature is presently not available in RF-ID tags and would require non-trivial modifications to the electronic chip and RF-ID tag reader. In addition, the absence of an electronic chip allows a passive materials tag to be relatively thin and environmentally robust.

	RF-ID TAG	MATERIALS TAG
cost per tag (low end)	~$.90	$.01
read range	limited by IC chip	slightly farther
# of ID bits per tag (based on 5cm X 5cm area)	10-100 is common	12 bits is challenging (limited by area)
sensing capability	not yet available	YES
ability to write data	YES (32 bits not difficult)	no good mechanism yet (few bits may be possible)
resistance to damage	moderate	high
reader complexity	less complex	more complex

Table 1. Comparison of RF-ID and passive materials tag technologies.

C. Long-Range Tags

This document has focused mostly on tags which operate via near-field coupling to a dipole antenna. However, for completeness, it is worth mentioning that there exists another growing class of wireless tags which are made to operate at longer distances (> 2 m). They are also known as far-field tags, and have also been used in EAS systems. This class of tag does not produce any electric or magnetic dipole signal, but rather function by periodically scattering or reflecting the signal transmitted by the tag reader. As one might suspect, these tags operate at much higher frequencies (>.9 GHz) and are powered by a battery or by a field in the vicinity of the tag.

Far-field tags are basically active antennas which modulate their scattering cross-section as a means of identifying themselves. In the past, most types of simple active antennas and active repeaters have existed in the realm of military surveillance or for simple tracking of wild animals such as butterflies, but we are now starting to see some types of far-field tags available in the commercial market (made by Micron, Phillips, for example). For long range tagging applications, we will also explore far-field scattering antennas and investigate the use of smart material antenna structures.

D. Future Vision

Electromagnetic tagging is an electronic interface technology, which enables electronic appliances to interact with people and objects in the physical environment. Like other interface technologies, future tagging systems will be more unobtrusive and easier to use. As appliances begin to use more forms of electromagnetic physical mechanisms, tagging will be seamlessly integrated with other interface technologies.

Our perception of a computers will change, so "a computer" doesn't mean a box that sits on your desk that you type on, but rather a computer will become a distributed

intelligence that it integrated into all the electronic appliances in our home or office. Because appliances can be wirelessly networked together, and because we will be able to interact with computers using just the everyday objects around us, the type of self-contained isolated computer which we know today will be in the minority.

Electromagnetic tagging is only a part – but a very essential part – of adding functionality, efficiency, and convenience to the spaces in which we live and work. Low cost electromagnetic tagging makes these benefits accessible to a much wider variety of consumer products. Shoes that can store information, doorknobs that know who is touching them, and refrigerators that know their contents are just some of the products we will see in the near future. We achieve this by applying physics, material science, and chemistry to make connections between the physical and digital worlds.

Not everyone in this world can program a computer (or afford one), and much of the world's population has never used a telephone, but most people know how use a pair of shoes, a chair, or a coffee mug. By instilling everyday objects with some of the intelligence afforded by modern-day computers, we can make useful electronic objects – things that think – which will increase the increase the efficiency of our work, improve the quality of our lives, and enable a larger fraction of the world to share in the benefits of technology.

References

[Butterworth] S. Butterworth and F. Smith; *Proc. Phys. Soc.*, Vol. 43, 1931, p. 166.

[Collin] R. E. Collin; *Foundations for Microwave Engineering*, McGraw-Hill, 1992.

[Fletcher] R. Fletcher, J. Cook; *Measurement of Surface Impedance vs. Temperature Using a Generalized Sapphire Resonator Technique*; Rev. of Scientific Instruments, Vol. 65 No. 8, Aug 1994, pp 2658-2666.

[Ginzton] E. Ginzton, Microwave Measurements, McGraw-Hill, 1957.

[Haus] H. Haus, J. Melcher; *Electromagnetic Fields and Energy*, Prentice Hall, 1989.

[Kajfez1] D. Kajfez, P. Guillon (eds); *Dielectric Resonators*, Vector Fields, 1990.

[Kajfez2] D. Kajfez; *Correction for Measured Unloaded Frequency of Cavity*, Electronics Letters, 19 Jan 1984, Vol. 20, No. 2, p. 81.

[Kajfez3] D. Kajfez, E. Hwan; *Q-Factor Measurement with Network Analyzer*, IEEE Trans. Microwave Theory and TechniquesElectronics, Vol. MTT-32, No. 7, July 1984

[Kajfez4] D. Kajfez; *Q-Factor*, Vector Fields, 1994.

[Mermerlstein1] M. Mermelstein; *IEEE Trans. Mag.*, Vol. 22, 1986, p. 442

[Mermerlstein2] M. Mermelstein; *IEEE Trans. Mag.*, Vol. 28, 1992, p. 36
Volume 2, Polytechnic Press, 1963.

[O'Handley1] R. O'Handley; *Magnetic Materials: Principles and Applications*, John Wiley and Sons, 1998.

[O'Handley2] R. O'Handley; Magnetic Materials for EAS Sensors, Journal of Materials Engineering and Performance, Vol. 2(2), April 1993, p. 211.

[Plonsey] R. Plonsey, R. E. Collin; *Principles and Applications of Electromagnetic Fields*, 1961, p. 336-341.

[Reitz] J. Reitz, F. Milford, R. Christy; *Foundations of Electromagnetic Theory*, 3rd Edition, Addison-Wesley, 1979.

[Staelin] D. Staelin, A. Morgenthaler, J. A. Kong; *Electromagnetic Waves*, Prentice-Hall 1994.